Long-term incubations provide insight into the mechanisms of anaerobic oxidation of methane in methanogenic lake sediments

Hanni Vigderovich[a], Werner Eckert[b], Michal Elul[a], Maxim Rubin-Blum[c], Marcus Elvert [d], Orit Sivan[a]

[a] Department of Earth and Environmental Science, Ben-Gurion University of the Negev, Beer Sheva, Israel
[b] Israel Oceanographic & Limnological Research, The Yigal Allon Kinneret Limnological Laboratory, Israel
[c] Israel Oceanographic & Limnological Research, Haifa, Israel
[d] MARUM - Center for Marine Environmental Sciences and Faculty of Geosciences, University of Bremen, Bremen, Germany

Corresponding author: Hanni Vigderovich, hannil@post.bgu.ac.il

Abstract

Anaerobic oxidation of methane (AOM) is ~~one of~~among the ~~major~~main processes limiting the release of the greenhouse gas methane from natural environments. ~~In Lake Kinneret (Israel), geochemical~~Geochemical profiles and experiments with fresh sediments from Lake Kinneret (Israel) indicate that iron-coupled AOM (Fe-AOM) sequesters 10-~~-~~15% of the methane produced in the methanogenic zone (> 20-~~-~~cm sediment depth). The oxidation of methane in this environment was shown to be mediated by a combination of *mcr* gene-bearing archaea and *pmoA* gene-bearing aerobic bacterial methanotrophs. Here, we ~~aimed~~used sediment slurry incubations under controlled conditions to ~~investigate~~elucidate the ~~AOM process in terms of various~~ electron acceptors and ~~involved~~ microorganisms ~~during~~that are involved in the AOM process over long-term ~~anaerobic sediment slurry incubations (~~(~18 months~~) under controlled conditions.~~). We ~~followed~~monitored the process with the addition of ^{13}C-labeled methane and two stages of incubations: (i) enrichment of the microbial population involved in AOM and (ii) slurry dilution and manipulations, including the addition of ~~multiple~~several electron acceptors (metal oxides, nitrate, nitrite and humic substances) and inhibitors ~~for~~ (2-bromoethanesulfonate, acetylene and sodium molybdate) of methanogenesis~~/AOM~~, methanotrophy and sulfate reduction~~./~~sulfur disproportionation. Carbon isotope measurements in the dissolved inorganic carbon pool ~~in these long-term incubations~~ suggest ~~that considerable~~the persistence of AOM ~~consumed~~, consuming 3-~~-~~8% of the methane produced at a rate of 2.0±0.4 nmol ~~g~~rg^{-1} dry sediment day^{-1}. ~~Carbon isotope measurements in lipids~~Lipid carbon isotopes and metagenomic analyses ~~indicate that only anaerobic~~point towards methanogens as the sole microbes ~~catalyzed this AOM. Whereas cryptic oxidation of methane~~performing the AOM process by ~~combining archaea and aerobic methanotrophs is feasible in the natural Lake Kinneret sediments,~~ reverse methanogenesis ~~dominates methane turnover in the long-term controlled experiments.~~. Humic substances and iron oxides, but not sulfate, manganese, nitrate, ~~and~~or nitrite, are the likely electron acceptors used ~~during the~~for this AOM. Our observations support the contrast between methane oxidation mechanisms in naturally anoxic lake

sediments, with potentially co-existing aerobes and anaerobes, and long-term incubations, ~~where~~wherein anaerobes prevail.

Keywords: Anaerobic oxidation of methane (AOM), lake~~,~~ sediments, dissolved inorganic carbon, stable carbon isotopes, electron ~~acceptor~~acceptors, archaea, methanogens, methanotrophs, lipids.

1. Introduction

Methane (CH_4) is an ~~effective~~important greenhouse gas (Wuebbles and Hayhoe, 2002) ~~with~~, which has both anthropogenic and natural sources~~. Natural methane sources contribute~~, the latter of which account for about 50% of ~~this gas~~the emission of this gas to the atmosphere (Saunois et al., 2020). ~~Aerobic~~Naturally occurring methane is mainly produced biogenically via the methanogenesis process, which is performed by methanogenic archaea. Traditionally acknowledged as the terminal process anchoring carbon remineralization (Froelich et al. 1979), methanogenesis occurs primarily via the reduction of carbon dioxide by hydrogen in marine sediments and via acetate fermentation in freshwater systems (Whiticar et al. 1986).

Methanotrophy, the aerobic and anaerobic oxidation of methane (AOM) by microbes, naturally ~~control~~controls the release of this gas to the atmosphere (Conrad, 2009; Reeburgh, 2007; Knittel and Boetius, 2009). In marine sediments, up to 90% of the upward methane flux is consumed anaerobically by sulfate, and in established diffusive profiles, that methane consumption occurs within a distinct sulfate-methane transition zone (Valentine 2002). While sulfate-dependent AOM, catalyzed by the archaeal ANaerobic MEthanotrophs (ANMEs) 1-3, is widespread ~~mostly~~chiefly in marine sediments (Hoehler et al., 1994; Boetius et al., 2000; Orphan et al., 2001; Treude et al., 2005, 2014), methane oxidation in other environments ~~methane oxidation~~ can be coupled to other electron acceptors~~.~~

~~AOM coupled to the reduction of iron~~ (e.g. Raghoebarsing et al., 2006; Ettwig et al. 2010; Sivan et al., 2011; Crowe et al. 2011; Norði and ~~manganese oxides has been confirmed in several environments (Beal et al., 2009; Egger et al., 2015; Sivan et al., 2011; Sivan et al., 2014; Segarra et al., 2013; Bar-or et al., 2017; Aromokeye et al., 2020; Su et al., 2020~~Thamdrup 2014~~;~~ ~~Mostovaya et al., 2021).~~ ~~Alternative electron acceptors for AOM include other metals, humic substances, nitrate and nitrite. The synthetic analog for humic substances, 9,10-anthraquinone-2,6-disulfonate (AQDS), was shown to serve as a terminal electron acceptor (Scheller et al., 2016;~~ Valenzuela et al., 2017).

In freshwater sediments sulfate is often depleted, and methanogenesis may be responsible for most of the organic carbon remineralization, resulting in thus high concentrations of methane in shallow sediments (Sinke et al., 1992). Indeed, lakes and wetlands, are responsible for 33-55% of naturally

emitted methane (Rosentreter et al., 2021). A large portion of this produced methane is oxidized by aerobic (type I) methanotrophic bacteria via oxygen. Aerobic methanotrophy is generally observed in the sediment-water interface (Damgaard et al. 1998) and/or in the water column thermocline (Bastviken 2009). AOM, however, can also consume over 50% of the produced methane (Segarra et al. 2015).

Sulfate can be an electron acceptor of AOM in freshwater sediments, as was shown for example in Lake Cadagno (Schubert et al., 2011, Su et al., 2020). Alternative electron acceptors for AOM in natural freshwater environments and cultures include humic substances, nitrate, nitrite and metals (such as iron manganese and chromium). Natural humic substances and their synthetic analogs were shown to function as terminal electron acceptors for AOM in soils, wetlands and cultures (Valenzuela et al., 2017; 2019; Bai et al., 2019; Zhang et al., 2019; Fan et al., 2020). Nitrate-dependent AOM has been demonstrated in a consortium of archaea and denitrifying bacteria from a canal (Raghoebarsing et al., 2006) and in an, in freshwater lake sediments (Norði and Thamdrup 2014) and in a sewage enrichment culture of ANME-2d (Haroon et al., 2013; Arshad et al., 2015), whereas nitrite fuels AOM by *Methylomirabilis* (NC-10, . Nitrite is exploited to oxidize methane by the aerobic bacteria *Methylomirabilis* (NC-10), which split the nitrite to N_2 and O_2 and then uses the produced oxygen to oxidize the methane (Ettwig et al., 2010). ANME-2d were also suggested to be involved in Cr(VI) coupled AOM, either alone or with a bacterial partner (Lu et al., 2016). Iron and/or manganese coupled AOM have also been suggested in lakes (Sivan et al., 2011; Crowe et al. 2011; Norði et al., 2013), sometimes by supporting sulfate-coupled AOM (Shubert et al., 2011; Su et al., 2020; Mostovaya et al., 2021). and *Methylomirabilis* can also couple AOM to selenite reduction (Luo et al., 2018). The ubiquitous aerobic methanotrophs Methylococcales may oxidize methane and denitrify under hypoxiaIron-coupled AOM was also shown to occur in enriched, denitrifying cultures from sewage where it was performed by ANME-2 (Ettwig et al. 2016), and in a bioreactor with natural sediments (Cai et al., 2018). (Kits et al., 2015), switch to iron reduction (Zheng et al., 2020), or generate oxygen by methanobactins (Dershwitz et al., 2021). The latter study also showed the ability of alphaproteobacterial methanotroph *Methylocystis* sp. strain SB2 to couple methane oxidation and iron reduction.

InThe mechanism and role of iron-coupled AOM in lake sediments have been studied with a variety of tools in the sediments of Lake Kinneret sediments, *in*. *In*-*situ* pore water profiles and top core experiments (Sivan et al., 2011), diagenetic models (Adler et al., 2011) and batch incubation experiments with fresh sediment slurries (Bar-Or et al., 2017) suggest that iron reduction coupled to AOM (Fe-AOM) removes 10-15% of the produced methane in the deep methanogenic zone (> 20 cm below the water-sediment interface). Analysis of the microbial community structure revealedsuggested that both methanogenic archaea and methanotrophic bacteria are potentially involved in methane oxidation (Bar-Or et al., 2015). Analyses of stable isotopes in fatty acids, the 16S rRNA gene amplicons and metagenomics showed that both reverse methanogenesis by archaea and the bacterial type I aerobic

methanotrophy by Methylococcales play ~~a~~important role in methane cycling (Bar-Or et al., 2017; Elul et al., 2021). ~~This aerobic methanotrophic activity~~Aerobic methanotrophy, which has also been observed in ~~several anoxic hypolimnions~~the hypolimnion and sediments of several other lakes that are considered anoxic (Beck et al., 2013; Oswald et al., 2016; Martinez-Cruz et al., 2017; Cabrol et al., 2020), may be driven by the presence of oxygen at nanomolar levels (Weng et al., 2018). Pure cultures of the ubiquitous aerobic methanotrophs Methylococcales have indeed been shown to survive under hypoxia either by oxidizing methane and with nitrate (Kits et al., 2015), ~~and might be fueled by the presence of oxygen at microlevel up to several meters below the oxycline. However, whether these methanotrophs continue to oxidize methane under strictly anoxic conditions and which electron acceptors are available is still unknown~~by switching to iron reduction (Zheng et al., 2020), or even by exploiting their methanobactins to generate their own oxygen to fuel their methanotrophic activity (Dershwitz et al., 2021). The latter study also showed that the alphaproteobacterial methanotroph *Methylocystis* sp., strain SB2, can couple methane oxidation and iron reduction. However, whether these aerobic methanotrophic bacteria are able to oxidize methane under strictly anoxic conditions and which electron acceptors are available to facilitate that activity are still not known.

~~Here, we used long-term anaerobic incubations to assess the dynamics of methane-oxidizing microbes under anoxic conditions and to quantify various electron acceptors' availability for AOM. For this purpose, we diluted fresh methanogenic sediments from Lake Kinneret with original porewater from the same depth and amended the sediment with ^{13}C-labeled methane, following its oxidation to dissolved inorganic carbon (DIC). Our experiment design consisted of two stages, the first stage included the enrichment of the microbial population involved in AOM, and the second stage involved an additional slurry dilution and several manipulations with multiple electron acceptors and inhibitors. The potential electron acceptors were iron and manganese oxides, nitrate, nitrite and humic substances. We inhibited the *mcr* gene with 2-bromoethanesulfonate (BES), methanogens with acetylene and sulfate reduction and sulfur disproportionation with Na-Molybdate (Nollet et al., 1997; Oremland & Capone, 1988; Lovley & Klug, 1983). We measured methane oxidation rates (by the ^{13}C-DIC enrichment), the electron acceptor characteristics (by their addition or inhibition) and the evaluated changes in microbial diversity over various incubation periods (based on metagenomics and lipid biomarkers). The results from the long-term anaerobic incubations were compared to those of batch and semi-bioreactor experiments that were set up with fresh sediments to follow the changes in methane oxidation mechanisms.~~

In the current study, we used long-term anaerobic incubations to assess the dynamics of methane-oxidizing microbes under anoxic conditions and to quantify the respective availabilities of different electron acceptors for AOM. To that end, we diluted fresh methanogenic sediments from Lake Kinneret with original porewater from the same depth and amended the sediment with ^{13}C-labeled methane. Our experiment design comprised two stages, the first of which included the enrichment of the microbial

population involved in AOM, while the second involved an additional slurry dilution and several manipulations with different electron acceptors and inhibitors. We measured methane oxidation rates (based on ^{13}C-DIC enrichment), determined the characteristics of each electron acceptor (via its turnover), and evaluated changes in microbial diversity over various incubation periods (based on metagenomics and lipid biomarkers). The results from the long-term anaerobic incubations were compared to those of batch and semi-continuous bioreactor experiments.

2. Methods

2.1 Study site

Lake Kinneret (Sea of Galilee) is a warm, monomictic, freshwater lake ~~located in the North of Israel. The lake~~that is 21 km long and 13 km wide~~.~~ and located in northern Israel. Its maximum depth is ~42 m at ~~the lake~~its center (station A, Figure S1) ~~and the~~while its average depth is 24 m. ~~The~~ From March to December, the lake is thermally stratified, and from ~~March~~April to December, ~~with~~ the hypolimnion ~~turning~~is anoxic ~~from April~~. Surface water temperatures range from 15 ~~to 30 °C, and~~ °C in the winter (January) to 32°C in the summer (August), while the lake's bottom water temperatures remain ~~between~~ in the range of 14-17 ~~°C all~~°C throughout the year ~~long. The lake sediments are composed mostly of carbonates (40-50%) and clays (20%; Hadas and Pinkas, 1995; Eckert, 2000). The total iron content in the top 40 cm of the sediments is ~3 wt % (Serruya, 1971; Eckert, 2000; Bar-Or et al., 2017).~~. The sediment ~~at~~from the deep methanogenic zone used in this study ~~(~20 cm~~ (sediment samples taken from a sediment depth of ~20 cm from the water-sediment interface at the lake's center) contains 50% carbonates, 30% clay and 7% iron (Table S1). The ~~porewater's~~ dissolved organic carbon (DOC) concentration of the porewater increases with depth, ranging from ~6 mg C L^{-1} at the sediment-water interface to 17 mg C L^{-1} at ~~25 cm~~a depth of 25 cm (Adler et al., 2011). ~~Dissolved methane~~ The concentrations of dissolved methane in the sediment porewater increase sharply ~~from the top sediments to~~with sediment depth, reaching a maximum of more than 2 mM at a depth of 15 cm ~~depth and then decrease~~, after which the amounts of dissolved methane gradually decreased with depth to 0.5 mM at a depth of 30 cm (Adler et al., 2011; Sivan et al., 2011; Bar-Or et al., 2015).

2.2 Experimental ~~set-up~~setup

~~This study compares three incubation strategies (A, B and C) of Lake Kinneret methanogenic sediments amended with original porewater from the same depth, ^{13}C-labeled methane, different potential electron acceptors for AOM (nitrite, nitrate, metal oxides and humic substances) and inhibitors for sulfur cycling and methanogens' activity (Fig. 1):~~

~~A) Long-term~~2.2.1 General

In this study we compared three incubation strategies (A, B and C; Fig. 1) in Lake Kinneret methanogenic sediments (sediment depths > 20 cm), which were amended with original porewater from

the same depth, ^{13}C-labeled methane, different potential electron acceptors for AOM (nitrite, nitrate, iron and manganese oxides and humic substances) and activity inhibitors. We inhibited the *mcr* gene with 2-bromoethanesulfonate (BES), methanogenesis and methanotrophy with acetylene, and sulfate reduction and sulfur disproportionation with Na-Molybdate (Nollet et al., 1997; Oremland & Capone, 1988; Lovley & Klug, 1983). Below we describe the three incubation strategies (Fig. 1).

A) Long-term, two-stage slurry incubations with a ~~first stage of~~ 1:1 sediment to porewater ratio ~~for three months with~~ and high methane content ~~to enrich~~for the first three months (first stage) to ensure the enrichment of the microorganisms involved in ~~the~~ AOM. After three months, the slurry was diluted with porewater to a 1:3 ratio~~, then~~ (second stage) and different reactants were added to the incubations, which were subsequently monitored for up to 18 months.

B) Semi-continuous bioreactor experiments ~~with~~ in which sediments were collected up to three days before the experiment was set up (freshly ~~collected~~sampled sediments) and sediment to porewater ~~at a 1:4~~ ratio ~~(respectively),~~of 1:4, where porewater was exchanged regularly.

C) Batch incubation experiments with ~~fresh~~freshly sampled sediments and porewater at a 1:5 ratio, respectively, and ~~several manipulations (this~~amended with hematite. This experimental set-up was described in our previous studies (Bar-Or et al., 2017; Elul et al., 2021~~)).~~).

~~Here below we describe the experiments. Detailed protocols are found in the supplementary information.~~

~~2.2.1 Experiment set-up A: Long-term two-stage incubations~~

The sediments for the slurries conducted in the current work were collected during ~~several~~seven sampling campaigns aboard the research vessel *Lillian* between 2017 and 2019 from the ~~central~~ center of the lake (Station A, Fig. S1) using a gravity corer with a 50~~-~~cm Perspex core liner. The length of the sediment in each core was 35-45 cm. During each sampling campaign, 1-2 sediment cores~~.~~ were collected for the incubations and 10 cores were collected for the porewater extraction. Sediments from the methanogenic zone ~~(>~~ (sediment depths > 20~~-~~cm ~~depth~~) were diluted with porewater from the methanogenic zone of parallel cores sampled on the same day. The porewater was extracted on the day of sampling. The sediment cores were sliced while onboard, and sediment samples from the methanogenic zone (> 20 cm) were transferred to a dedicated container. In the lab, sediments were collected with 20-ml cutoff syringes and moved to 50-ml falcon tubes. The porewater was extracted by centrifugation at 9300 g for 15 ~~minutes,~~min at 4°C, filtered by 0.22~~-~~µM filters into 250~~-~~ml pre-autoclaved glass bottles, crimp-sealed with ~~a~~ rubber ~~stopper~~stoppers, and flushed for 30 ~~minutes~~min with N_2. The extracted porewater was kept under anaerobic conditions at 4 until its use. The sediments for the incubations were subsamples from the liners and diluted no later than three days after their

collection from the lake and treated further according to the experimental strategies described above (setup A or B).

2.2.2 Experiment type A set-up: Long-term two-stage incubations (henceforth referred to as "two-stage" for simplicity)

Experiment A comprised ten two-stage incubation experiments (experiment serial numbers (SN) 1-10; Table 1) with different treatments (electron acceptors/shuttling/inhibitors). In the first stage~~, the sediment was~~ (pre-incubation slurry), the sediment core was sliced under a N_2 atmosphere and sediments from depths > 20 cm were collected into zipper bags. The sediment was homogenized, and between 80-100 gr transferred into 250-ml glass bottles under continuous N_2 flushing. The sediments were diluted with the extracted porewater to create a 1:1 ~~ratio~~sediment to porewater slurry ~~in 250 ml glass bottles~~ with a headspace of 70-90 ml ~~under continuous N_2 flushing~~ (Fig. 1). The slurries were sealed with rubber stoppers and crimped caps and were flushed with N_2 (99.999%, MAXIMA, Israel) for 30 ~~minutes~~min. Methane (99.99%, MAXIMA, Israel) was injected using a gas-tight syringe for a final content of 20% in the headspace, where 10% of the injected methane was ^{13}C-labeled methane (99%, Sigma-Aldrich). When significant AOM activity was observed ~~by~~based on the increase of $\delta^{13}C_{DIC}$ after approximately three months (Fig. S2), some of the incubations were ~~either transferred to~~further diluted during the second stage of the experiments ~~or~~. The remainder of the incubations continued to be run with porewater exchange ~~and~~while the $\delta^{13}C_{DIC}$ values were monitored every three months.

~~This study presents ten sets of two-stage incubation experiments with different treatments (electron acceptors/shuttling/inhibitors). They were all~~All the experiments were set up similarly (see dates and detailed protocols in the supplementary information): the pre-incubation bottle was opened and subsamples (~18 g each) ~~of the pre-incubation slurry~~ were transferred with a syringe and a Tygon® tube under a laminar hood and continuous flushing of N_2 gas into 60~~-~~-ml glass bottles~~ and~~. The subsamples were then diluted with fresh anoxic porewater from the methanogenic zone (as described above) to achieve a 1:3 sediment to porewater ratio (Fig. 1~~),~~) while leaving 24 ml of headspace in each ~~experiment~~ bottle. The bottles were crimp-sealed, flushed with N_2 gas for 5 ~~minutes~~min, shaken vigorously and flushed again (3 times). Then ^{13}C-labeled methane was added to all of the bottles as described in Table 1. The "killed" control ~~bottles~~slurries in each experiment were autoclaved twice~~,~~ and cooled, ~~and~~ only ~~then~~after which they were amended with the appropriate treatments and ^{13}C-labeled methane.

~~Electron~~To the diluted (1:3) batch slurries electron acceptors were added either as a powder (hematite – experiment no. 1, magnetite – experiment no. 2, clay~~, MnO_2,~~ and humic substances – experiment no. 7, MnO_2 – experiment no. 3) or in dissolved form in double-distilled water (DDW) (KNO_3 ~~and~~ – experiment no. 4, $NaNO_2$ – experiment no. 5). ~~). The~~ In addition, the potential involvement of sulfur cycling in the transfer of electrons was tested ~~by~~in experiment no. 2 via its inhibition with Na-molybdate

(Lovley and Klug, 1983)~~, while the other electron acceptors were tested for their potential participation by their addition to the slurries. AQDS was added as an~~. The synthetic analog for humic substances, ~~which was previously shown to serve as a terminal electron acceptor for AOM~~i.e., 9,10-anthraquinone-2,6-disulfonate (AQDS), was dissolved in DDW (detailed in the supplementary information) and ~~electron shuttling for iron reduction (e.g., Scheller et al., 2016; Sivan et al., 2016).~~added to the bottles of experiment no. 6 until a final concentration of 5 mM was achieved in each bottle. Amorphous iron ($Fe(OH)_3$) was prepared in the lab by dissolving $FeCl_3$ in DDW~~,~~ that was then titrated with NaOH 1.5 N up to pH 7 and ~~was added~~injected to the bottles ~~by injection~~of experiment no. 2 . The final concentration of each addition is detailed in Table 1. The ^{13}C-labeled methane was injected ~~to~~into all ~~experiment~~ of the experimental bottles at the beginning of each experiment (unless ~~mentioned~~described otherwise) by using a gas-tight syringe from a stock bottle filled with ^{13}C-labeled methane gas (which was replaced with saturated NaCl solution). Three different inhibitors were added to three different experiments: ~~molybdate, BES and acetylene.~~ Molybdate was added to experiment No. ~~1~~1 (to one bottle of methane-only treatment, magnetite treatment and amorphous iron treatment) to detect the feasibility of an active sulfur cycle~~.~~; BES was added to experiment No. 8 at the start of the experiment~~. Acetylene~~; and acetylene was added to experiment No. 9~~. It~~, wherein it was injected during the experiment ~~to~~into two bottles at different timepoints after ^{13}C enrichment ~~in the DIC~~ was observed in the DIC (Table 1).

All live treatments were set up in ~~duplicates~~duplicate or ~~triplicates and we present~~ triplicate, depending on the amount of the pre-incubated slurry aimed for each experiment, and the results are presented as the average with an error bar. In two experiments, only one "killed" control bottle was set up~~. The~~, and the remainder of the slurry was prioritized for other treatments ~~since~~, because the killed controls repeatedly showed ~~repetitive~~ no activity ~~for numerous~~in several previous experiments. The humic substrate experiment used a natural (humic) substance that ~~were~~was extracted from a ~~different~~ lake near Fairbanks, Alaska, where the iron reduction was observed in the methanogenic zone. One experiment was set up without any additional electron acceptor to assess the rate of methanogenesis in the two-stage slurries. Porewater was sampled anaerobically for $\delta^{13}C_{DIC}$ and dissolved Fe(II) measurements in ~~duplicates~~duplicate (2 ml), and methane was measured from the headspace. Variations in the $\delta^{13}C_{DIC}$ values between the experiments resulted from different amounts of ^{13}C~~-~~-labeled methane injected at the start of each experiment~~.~~ (geochemical measurements detailed in the analytical methods section below).

2.2.~~2~~3 Experiment ~~set-up~~type B setup: Semi-continuous bioreactor

Semi-continuous bioreactors ~~regularly monitored~~were used to monitor the redox state regularly at close-to-natural *in-situ* conditions for 15 months in freshly collected sediments. Two 0.5~~-~~-L semi-continuous bioreactors (Fig. 1) (LENZ, Weinheim, Germany) were set up with ~~fresh~~freshly sampled sediments from the methanogenic zone (25 - 40 cm) ~~of~~and extracted porewater from the same depth from Station A on Lake Kinneret ~~Station A~~ immediately after their collection. Both reactors were filled, headspace-

free, with a slurry at a 1:4 sediment ~~- pore water~~to porewater ratio. One ~~of the bioreactors~~bioreactor was amended with 10 mM hematite ~~and~~while the second ~~without it, serving as~~, which was a control, was not amended. To dissolve ^{13}C-labeled methane in the porewater, 15 ml of porewater were replaced with 15 ml of methane gas (~~a mixture~~13 ml of $^{12}CH_4$ and 2 ml of $^{13}CH_4$) to produce a methane-only headspace for 24 ~~hours. The~~ h, during which time the reactors were shaken repeatedly ~~during those hours.~~. After 24 ~~hours~~ h, the gas was replaced with anoxic porewater, ~~so that there was no~~thus eliminating the headspace ~~at all. This~~, which resulted in lower methane concentrations (0.2 mM) than ~~the~~in either the two-stage incubations or the fresh batch ~~experiments (0.2 mM vs. ~2 mM, respectively). Redox~~experiment (~2 m). The redox potential was monitored continuously ~~by~~using a platinum/glass electrode (Metrohm, Herisau, Switzerland) to verify anoxic conditions and to determine the redox state throughout the incubation period. The bioreactors were subsampled weekly to bi-weekly, and the sample volume (5-10 ml) was replaced immediately by preconditioned anoxic (flushed with N_2 gas for 15 ~~minutes~~min) porewater from the methanogenic zone. As outlined below, samples were analyzed for dissolved Fe(II), ~~CH_4,~~methane and $\delta^{13}C_{DIC}$. Additional subsamples for metagenome and lipid analyses were taken at the beginning of the experiment and on days 151 and 382, respectively.

2.2.~~3~~4 Experiment ~~set-up~~type C setup: Fresh batch experiment

Sediments for this experiment were collected in August 2013 at Station A~~,~~ using a protocol similar to that used to collect the sediments for the pre-incubations. ~~The sediments below~~Sediments from depths greater than 26 cm ~~depth~~ were diluted under anaerobic conditions with porewater from the same depth to ~~reach~~obtain a ~~1:5~~ratio of sediment to porewater ~~ratio~~of 1:5. The resulting slurry was then divided ~~into~~between 60 ~~-~~ml ~~experiment~~glass bottles ~~with~~ (40 ml slurry in each bottle~~.~~). The sampling and experimental ~~set-up details~~setup are described in detail in our earlier study (Bar-Or et al., 2017~~.~~). Here we present ~~the~~our results of the $\delta^{13}C_{DIC}$, metagenome and lipid analyses of two treatments: natural (with only ^{13}C-labeled methane) and hematite. The experiment ran for 15 months.

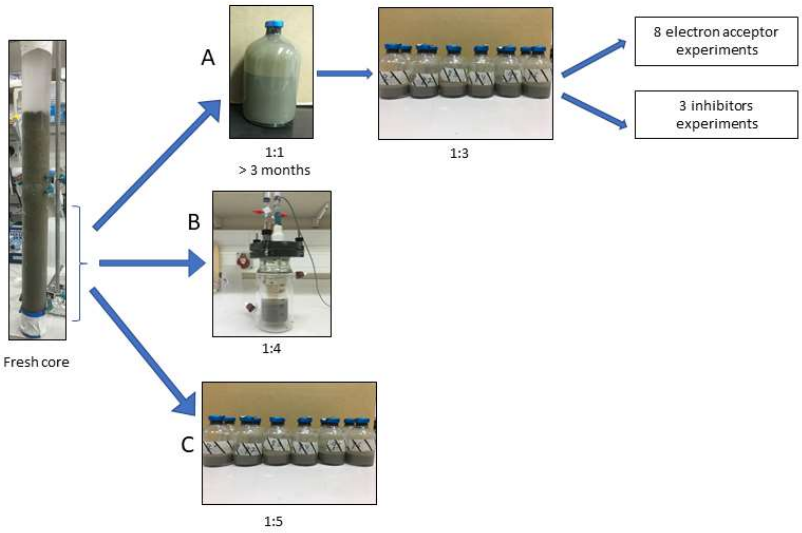

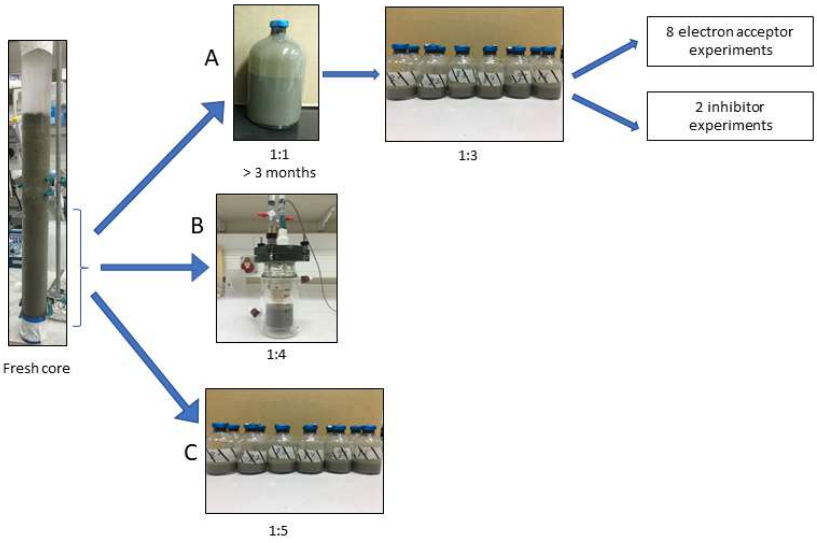

Figure 1: Flow diagram of the experimental design. Three types of experiments were set up ~~from sediments of~~ to investigate the methanogenic zone ~~(below~~sediments (deeper than 20 cm): **A**~~.~~) Two-stage slurry experiments, with 1:1 ratio of sediment to porewater incubations and then with diluted pre-incubated slurries and porewater (1:3 ~~sediment to porewater ratio). Ten experiments were set up this way, 8~~ratio of ~~them with different electron acceptors for 6–18 months, and three different inhibitors for 12–18 months (to one experiment, both electron acceptors and an inhibitor were added).~~sediment to porewater). **B**~~.~~) Semi-aerobic bioreactor experiment with

freshly collected ~~sedimentssediment~~. C.) Fresh batch experiment –– slurry experiment with freshly collected sediments (Bar-Or et al., 2017).

Experiment serial number (SN)	Experiment	Treament	# of bottles	CH_4 [ml]	$^{13}CH_4$ [ml]	Fe_2O_3 [mM]	Fe_3O_4 [mM]	$Fe(OH)_3$ [mM]	MnO_2 [mM]	NO_2^- [mM]	NO_3^- [mM]	AQDS [mM]	Humic substances [mM]	PCA [mM]	Fe-bearing montronite (clay) [gr]	Na_2-molybdate [mM]	BES [mM]	Acetylene [µL]	Temp [c°]	Duration [day]	Comments
1	Hematite	$^{13}CH_4$	2		1														20	201	
		$^{13}CH_4$+hematite	2		1	10													20		
2	Magnetite	$^{13}CH_4$	2		1											1			16	447	The methane that was added at the beginning of the experiment was not labelled, so ^{13}C-labeled methane was added after 105 days. Na_2-molybdate was added to one of the bottles on day 365
		$^{13}CH_4$+magnetite	2		1		10									1			16		Na_2-molybdate was added to one of the bottles on day 365
		$^{13}CH_4$+$Fe(OH)_3$	2		1			10								1			16		
		Killed+$^{13}CH_4$+magnetite	1		1		10												16		
3	MnO_2	$^{13}CH_4$	2		1.2														20	201	200 µL $^{13}CH_4$ was added on day 1, then another 1 mL was added on day 24.
		$^{13}CH_4$+MnO2	2		1.2				10										20		200 µL $^{13}CH_4$ was added on day 1, then another 1 mL was added on day 24.
4	Nitrate	$^{13}CH_4$+NO_3^- (high conc.)	2	1	0.5	12					1								20	306	
		$^{13}CH_4$+hematite	2	1	0.5	12													20		
		$^{13}CH_4$+NO_3^- (high conc.)+hematite	2	1	0.5	12					1								20		
		$^{13}CH_4$+NO_3^- (low conc.)+hematite	2	1	0.5	12					0.2								20		
		Killed+$^{13}CH_4$+NO_3^- (high conc.)+hematite	1	1	0.5	12					1								20		
5	Nitrite	$^{13}CH_4$	3	1	0.5														20	493	
		$^{13}CH_4$+NO_2^- (high conc.)+hematite	2	1	0.5	10				0.5									20		
		$^{13}CH_4$+NO_2^- (low conc.)+hematite	2	1	0.5	10				0.1									20		
		Killed+$^{13}CH_4$+NO_2^- (high conc.)+hematite	2	1	0.5	10				0.5									20		
6	AQDS	$^{13}CH_4$	3		1														20	264	
		$^{13}CH_4$+AQDS	2		1							5							20		
		$^{13}CH_4$+AQDS+hematite	2		1	10						5							20		
		Killed+$^{13}CH_4$+AQDS	2		1														20		
7	Natural humic acids and clay	$^{13}CH_4$	2		1	10							0.5						20	169	The head space of the experiment bottles was flushed with N_2 on day 51 and $^{13}CH_4$ was added. This was done in order to match the the clay bottles.
		$^{13}CH_4$+hematite	2		1	10													20		
		$^{13}CH_4$+humic acid	2		1														20		
		$^{13}CH_4$+clay	2		1	10									1				20		Clay was added on day 43, and the bottles were flushed again with N_2. $^{13}CH_4$ was added again on day 51.
		Killed+$^{13}CH_4$+hematite	2		1	10													20		
8	Bromoethanesulfonate (BES)	$^{13}CH_4$+hematite	2	9	1	10													20	493	
		$^{13}CH_4$+hematite+BES	2	9	1	10											20		20		
9	Acetylene	$^{13}CH_4$+hematite	4	1	0.5	10												120	20	321	
		$^{13}CH_4$+hematite+acetylene	2	1	0.5	10												120	20		Acetylene was injected to each bottle at different time point doring the experiment.
		Killed+$^{13}CH_4$+hematite	2	1	0.5	10													20		
10	No electron acceptor	No additions	3																20	147	
		$^{13}CH_4$	3		1														20		
	Semi-bioreactor	$^{13}CH_4$		15															16	345	
		$^{13}CH_4$+hematite		15		10													16	677	
	Freshly collected sediment exp.	$^{13}CH_4$			0.05														20	467	
		$^{13}CH_4$+hematite			0.05	20													20		

311

Table 1: ~~Specific details~~Details of the three types of experiments: two-stage, semi-aerobic bioreactor and fresh batch experiments.

Experiment serial number (SN)	Experiment	Treatment	# of bottles	CH_4 [ml]	$^{13}CH_4$ [ml]	Fe_2O_3 [mM]	Fe_3O_4 [mM]	$Fe(OH)_3$ [mM]	MnO_2 [mM]	NO_2^- [mM]	NO_3^- [mM]	AQDS [mM]	Humic substances [mM]	PCA [mM]	Fe-bearing nontronite (clay) [gr]	Na_2-molybdate [mM]	BES [mM]	Acetylene [µL]	Temp [c°]	Duration [day]	Comments
1	Hematite	$^{13}CH_4$	2		1	10													20	201	
		13CH4+hematite	2		1	10													20		
2	Magnatite	$^{13}CH_4$	2		1		10									1			16	447	The methane that was added at the beginning of the experiment was not labeled, so ^{13}C-labeled methane was added after 105 days. Na_2-molybdate was added to one of the bottles on day 365
		$^{13}CH_4$+magnetite	2		1		10									1			16		Na_2-molybdate was added to one of the bottles on day 365
		$^{13}CH_4$+$Fe(OH)_3$	2		1			10											16		
		Killed+$^{13}CH_4$+magnetite	1		1		10												16		
3	MnO_2	$^{13}CH_4$	2		1.2														20	201	200 µL $^{13}CH_4$ was added on day 1, then another 1 mL was added on day 24.
		$^{13}CH_4$+MnO2	2		1.2				10										20		200 µL $^{13}CH_4$ was added on day 1, then another 1 mL was added on day 24.
4	Nitrate	$^{13}CH_4$+NO_2^-(high conc.)	2	1	0.5	12					1								20	306	
		$^{13}CH_4$+hematite	2	1	0.5	12													20		
		$^{13}CH_4$+NO_3^-(high conc.)+hematite	2	1	0.5	12					1								20		
		$^{13}CH_4$+NO_3^-(low conc.)+hematite	2	1	0.5	12					0.2								20		
		Killed+$^{13}CH_4$+NO_3^-(high conc.)+hematite	1	1	0.5	12					1								20		
5	Nitrite	$^{13}CH_4$	3	1	0.5														20	493	
		$^{13}CH_4$+NO_2^-(high conc.)+hematite	2	1	0.5	10				0.5									20		
		$^{13}CH_4$+NO_2^-(low conc.)+hematite	2	1	0.5	10				0.1									20		
		Killed+$^{13}CH_4$+NO_2^-(high conc.)+hematite	2	1	0.5	10				0.5									20		
6	AQDS	$^{13}CH_4$	3		1							5							20	264	
		$^{13}CH_4$+AQDS	2		1	10						5							20		
		Killed+$^{13}CH_4$+AQDS	2		1														20		
7	Natural humic acids and clay	$^{13}CH_4$	2		1	10							0.5						20	169	The head space of the experiment bottles was flushed with N_2 on day 51 and $^{13}CH_4$ was added. This was done to match the the clay bottles.
		$^{13}CH_4$+hematite	2		1	10													20		
		$^{13}CH_4$+humic acid	2		1										1				20		Clay was added on day 43, and the bottles were flushed again with N_2. $^{13}CH_4$ was added again on day 51.
		$^{13}CH_4$+clay	2		1	10													20		
		Killed+$^{13}CH_4$+hematite	2		1	10													20		
8	Bromoethanesulfonate (BES)	$^{13}CH_4$+hematite	2	9	1	10													20	493	
		$^{13}CH_4$+hematite+BES	2	9	1	10											20		20		
9	Acetylene	$^{13}CH_4$+hematite	4	1	0.5	10												120	20	321	Acetylene was injected to each bottle at different time points during the experiment.
		$^{13}CH_4$+hematite+acetylene	2	1	0.5	10												120	20		
		Killed+$^{13}CH_4$+hematite	2	1	0.5	10													20		
10	No electron acceptor	No additions	3																20	147	
		$^{13}CH_4$	3		1														20		
	Semi-bioreactor	$^{13}CH_4$		15															16	345	
		$^{13}CH_4$+hematite		15		10													16	677	
	Freshly collected sediment exp.	$^{13}CH_4$			0.05														20	467	
		$^{13}CH_4$+hematite			0.05	20													20		

2.3 Analytical methods

2.3.1 Geochemical measurements

Measurements of $\delta^{13}C_{DIC}$ were performed on a DeltaV Advantage Thermo Scientific isotope-ratio mass-spectrometer (IRMS). Results are reported referent to the Vienna Pee Dee Belemnite (VPDB) standard. For these measurements, about 0.3 ml of filtered (0.22 µm) porewater was injected into a 12-ml glass vial with a He atmosphere and 10 µl of H_3PO_4 85% to acidify all the DIC species to CO_2 (g). The headspace autosampler (CTC Analytics; Type PC PAL) took a sampled the gas sample from the vials and measured the $\delta^{13}C_{DIC}$ of the sample on the GasBench interface with a precision of ±0.1 ‰. DIC was measured on the IRMS using the peak height and a precision of 0.05 mM. Dissolved Fe(II) concentrations were measureddetermined using the ferrozine method (Stookey, 1970) by a spectrophotometer at a 562-nm wavelength with a detection limit of 1 µmol L^{-1}. Methane concentrations were measured from the headspace. A 100-µL headspace sample was taken for methane measurements with a gas-tight syringe and was analyzed by a focus gas chromatograph (Focus GC, Thermo) equipped with a flame ionization detector (FID) and a packed column (Shincarbon ST) with a helium carrier gas (UHP) and a detection limit of 0.005 µmol.1 nmol methane. Bottles to which acetylene was added were also measured similarlyby GC for ethylene to determine the acetylene turnover with the N cycle.

2.3.2 Lipid analysis

A sub-set of samples (Table 3) was investigated for the assimilation of ^{13}C-labeled methane into polar lipid-derived fatty acids (PLFAs) and intact ether lipid-derived hydrocarbons. A total lipid extract (TLE) was obtained from 0.4 to 1.6 g of the freeze-dried sediment or incubated sediment slurry using a modified Bligh and Dyer protocol (Sturt et al., 2004). Before extraction, 1 µg of 1,2-diheneicosanoyl-*sn*-glycero-3-phosphocholine and 2-methyloctadecanoic acid were added as internal standards. PLFAs in the TLE were converted to fatty acid methyl esters (FAMEs) using saponification with KOH/MeOH and derivatization with BF_3/MeOH (Elvert et al., 2003). Intact archaeal ether lipids in the TLE were separated from the apolar archaeal lipid compounds using preparative liquid chromatography (Meador et al., 2014) followed by ether cleavage with BBr_3 in dichloromethane forming hydrocarbons (Lin et al., 2010). Both FAMEs and ether-cleaved hydrocarbons were analyzed by GC-mass spectrometry (GC-MS; Thermo Finnigan Trace GC coupled to a Trace MS) for identification and by GC-IRMS (Thermo Scientific Trace GC coupled via a GC Isolink interface to a Delta V Plus) for determination ofto determine $\delta^{13}C$ values by using the column and temperature program settings described by Aepfler et al. (2019). The $\delta^{13}C$ values are reported with an analytical precision better than 1‰ as determined by long-term measurements of an *n*-alkane standard with known isotopic composition of each compound. Reported fatty acid isotope data are corrected for the introduction of the methyl group during

derivatization by mass balance calculation similar to equation 1 (see below) using the measured $\delta^{13}C$ value of each FAME and the known isotopic composition of methanol as input parameters.

2.3.3 Metagenomic analysis

For the metagenomic analyses, total genomic DNA was extracted from the semi-aerobic bioreactor ~~experiment (duplicates a and b~~with hematite addition (duplicate samples), pre-incubation slurries ($^{13}CH_4$-only control, $^{13}CH_4$ + hematite) and their respective initial slurries (t0~~),~~) by using the DNeasy PowerLyzer PowerSoil Kit (QIAGEN). Genomic DNA was eluted using 50 µl of elution buffer and stored at −20 °C. Metagenomics libraries were prepared at the sequencing core facility at the University of Illinois at Chicago using the Nextera XT DNA library preparation kit (Illumina, USA). Between 19- and 40 million 2 × 150 bp paired-end reads per library were sequenced using Illumina NextSeq500. Metagenomes were co-assembled from the concatenated reads of all of the metagenomic libraries with Spades V3.12 (Bankevich et al., 2012; Nurk et al., 2013~~), following~~) after decontamination, quality filtering (QV= 10) and adapter-trimming with the BBDuk tool from the BBMap suite (Bushnell B, http://sourceforge.net/projects/bbmap/). Downstream analyses, including reading coverage estimates, automatic binning with maxbin (Wu et al., 2014) and metabat2 (Kang et al., 2019) bin refining with the DAS tool (Sieber et al., 2018), were performed within the SqueezeMeta framework (Tamames and Puente-Sánchez, 2019). GTDB-Tk was used to classify the metagenome-assembled genomes (MAGs) based on Genome Taxonomy Database release 95 (Parks et al., 2021). The principal component analysis biplot was constructed with Past V4.03 (Hammer et al., 2001).

2.3.4 Rate calculations

Methanogenesis ~~rate was~~rates were calculated from temporal changes in methane concentration in a representative pre-incubated slurry experiment (Fig. ~~S3~~2). The amount of methane oxidized was calculated by a simple mass balance calculation according to equations 1 and 2:

$$x \times F^{13}CH_4 + (1 - x) \times FDI^{13}C_i = FDI^{13}C_f \quad \text{~~(1)~~(1)}$$

$$[CH_4]_{ox} = x \times [DIC]_f \quad (2)$$

The final DIC pool comprises two end members~~:~~, the initial DIC pool and the oxidized ^{13}C-CH_4. The term x denotes the fraction of oxidized ^{13}C-CH_4, while 1-x denotes the fraction of the initial DIC pool out of the final DIC pool. $F^{13}CH_4$ is the fraction of ^{13}C out of the total CH_4 at t0~~,~~ (i-initial), $FDI^{13}C_i$ is the fraction of ^{13}C out of the total DIC at t0, and $FDI^{13}C_f$ is the fraction of ^{13}C out of the total DIC at t~~-~~-final. $[CH_4]_{ox}$ is the amount (concentration in pore water) of the methane oxidized throughout the full incubation period, and $[DIC]_f$ is the DIC concentration at t-final. It was assumed that the isotopic composition of the labeled CH_4 did not change significantly throughout the incubation period.

3. Results

In ten sets of slurry incubation experiments, we followed the progress of the methane oxidation process in ~~(type A) long-term two-stage incubations from~~ Lake Kinneret methanogenic sediments ~~(Figs. 2 and 3)~~in type A two-stage long-term incubations. This is by monitoring the changes in $\delta^{13}C_{DIC}$ values~~,~~ and by running metagenomic and specific isotope lipid analyses. We also followed methane oxidation in a semi-continuous bioreactor system (type B) with freshly collected sediments with or without the addition of hematite (Fig. ~~2~~3). The results were compared to those of fresh batch slurry incubations (type C) from the same methanogenic zone, presented by Bar-Or et al. (2017) and Elul et al. (2021).

3.1 Geochemical trends in the long-term two-stage experiments

In the ~~two-~~second stage (1:3 ratio of sediment to porewater) long-term batch slurry experiments (type A~~),~~) from the methanogenic zone, methanogenesis occurred with net methanogenesis rates of ~ 25 nmol g dry weight $(DW)^{-1}$ d^{-1} (Fig. 2, Table S2), which are similar to those of fresh incubation experiments (Bar-Or et al., 2017). At the same time there was a conversion of ^{13}C-methane to ^{13}C-DIC in all the ~~natural~~ non-killed slurries amended with ^{13}C-methane, indicating significant AOM (Figs. ~~2~~3 and ~~3~~4). The $\delta^{13}C_{DIC}$ values of the ~~natural sediment amended only with ^{13}C-methane treatments (the "~~"methane-only~~"~~" control~~)~~ slurries reached ~~up to~~ as high values as 743~~‰, even with the low abundance of microbial populations in these sediments. Average~~‰. The average AOM rate in the methane-only controls was 2.0±0.4 nmol ~~gr~~g DW^{-1} ~~dry sediment day~~d^{-1} (Table 2). ~~At the same time, methanogenesis occurred with a net methanogenesis rate of ~ 25 nmol gr dry sediment^{-1} day^{-1} (Fig. S3, Table S2, Table 2.). The two-stage~~ AOM was observed in these geochemical experiments ~~tested first~~also with the addition of electron acceptors, and the potential of several electron acceptors to perform and stimulate the AOM process~~, as~~ is detailed below.

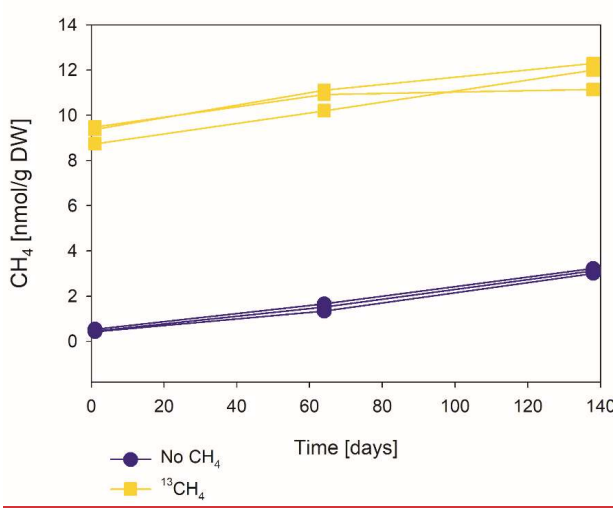

Figure 2: The change of methane concentrations with time of a representative incubated second stage long-term slurry experiment, showing apparent net methanogenesis with average rate of 25 nmol g DW^{-1} d^{-1}.

3.1.1 Metals as electron acceptors

Iron and manganese oxides were added as potential electron acceptors to the second stage long-term slurries. The addition of hematite to three different experiments increased the $\delta^{13}C_{DIC}$ values over time to 694‰, similar to the behavior of the methane-only controls, and in a different pattern than the fresh experiments (Fig. 3). The average AOM rate in those two-stage treatments was 1.0±0.3 nmol g DW^{-1} d^{-1} (Table 3). Magnetite amendments resulted in a minor increase of $\delta^{13}C_{DIC}$ values compared to the methane-only controls (200‰ and 265‰, respectively, Fig. 4A) with an AOM rate of 1.8 nmol g DW^{-1} d^{-1}. Amorphous iron amendments resulted in only a 22‰ increase in $\delta^{13}C_{DIC}$ and a lower AOM rate (0.1 nmol g DW^{-1} d^{-1}, Fig. 4A and Table 2). The addition of iron-bearing clay nontronite did not cause any increase in the $\delta^{13}C_{DIC}$ values (Fig. 4B), but the concentration of dissolved Fe(II) increased compared to the natural methane-only control (Fig. 5). Based on $\delta^{13}C_{DIC}$ estimates, no AOM was detected 200 days after the addition of MnO_2 whereas the $\delta^{13}C_{DIC}$ values of the methane-only controls increased to over 500‰ (Fig. 4F).

3.1.2 Sulfate as an electron acceptor

The involvement of sulfate in the AOM in the incubations was tested, even within the absence of detectable sulfate in the methanogenic sediments. This is as sulfate could theoretically still be a short living intermediate for the AOM process in an active cryptic sulfur cycle (Holmkvist et al., 2011). It was quantified directly by adding Na-molybdate to the methane-only controls and the amended with magnetite (in the second stage long-term incubations (Fig. 4A). This addition did not affect the increasing trend of $\delta^{13}C_{DIC}$ with time, and therefore, the AOM rates remained unchanged, similar to the observation in the fresh batch incubations (Bar-Or et al., 2017).

3.1.3 Nitrate and nitrite as electron acceptors

Nitrate and nitrite involvement in the AOM was tested for the feasibility of an active cryptic nitrogen cycle, even within the absence of detectable amounts of nitrate and nitrite in the sediments (Nüsslein et al., 2001; Sivan et al., 2011). Nitrate was added at two different concentrations (0.2 and 1 mM, Fig. 4C) to the second stage long-term slurries amended with hematite, as these concentrations were shown previously to promote AOM in other settings (Ettwig et al., 2010).

~~Hematite~~The addition of hematite alone increased the $\delta^{13}C_{DIC}$ values by ~200‰ during the 306 days of the experiment. The $\delta^{13}C_{DIC}$ in the bottles with the addition of 1 mM nitrate, with and without hematite (Fig. ~~3C~~4C; the data points of the two treatments are on top of each other~~)~~), decreased from 43‰ at the beginning of the experiment to 35‰ after 306 days. The $\delta^{13}C_{DIC}$ in the bottles with the addition of 0.2 mM nitrate and hematite increased by 27‰ at the end of the experiment. ~~We also~~Following the addition of 0.5 mM of nitrite, we observed no increase in $\delta^{13}C_{DIC}$ values during the first 222 days ~~following the addition of 0.5 mM of nitrite~~ (Fig. ~~3D), then $\delta^{13}C_{DIC}$~~4D), after which they increased from 34‰ to 54‰ by ~~19‰ until~~ the ~~incubation was terminated.~~end of the experiment. The ~~respective~~ AOM rate of the high nitrite concentration treatment was 0.2 nmol ~~gr dry sediment~~g DW^{-1} ~~day~~d^{-1} (Table 2). Following the addition of 0.1 mM nitrite, $\delta^{13}C_{DIC}$ increased only after 130 days ~~and reached~~to 158‰ ~~at~~on day 493. The ~~respective~~ AOM rate of the low nitrite concentration treatment was 0.5 nmol ~~gr dry sediment~~g DW^{-1} ~~day~~d^{-1}. In the methane-only controls, the $\delta^{13}C_{DIC}$ value reached a maximum of 330‰.

3.1.4 Organic compounds as electron acceptors

Two of the ~~two~~ second stage long-term incubation experiments were amended with synthetic and natural organic electron acceptors to test the potential of organic electron acceptors. The addition of AQDS to slurries with and without hematite ~~decreased the~~ caused to a decrease in $\delta^{13}C_{DIC}$ values ~~during~~over the entire duration of the experiment ~~duration~~ (Fig. ~~3E). The dissolved~~4E). Dissolved Fe(II) ~~showed an increase of~~ increased by 50 µM in these treatments, ~~whereas~~while in those without AQDS ~~there was~~, it exhibited an increase of 20 µM (Fig. ~~S4~~S3). We further tested the effect of naturally occurring humic substances by using those isolated from a different natural lake. The results show that the $\delta^{13}C_{DIC}$ values did not change at the beginning of the experiments (Fig. ~~3B~~4B), while a steep increase of ~90 µM in their Fe(II) ~~concentrations were~~concentration was observed (Fig. 45). After 20 days, the $\delta^{13}C_{DIC}$ values of these slurries started to increase dramatically from 84‰ to 150‰ with an AOM rate of 1.2 nmol ~~gr dry sediment~~g DW^{-1} ~~day~~d^{-1} (Fig. ~~3B~~4B, Table 2). ~~We observed a mirrored trend of the dissolved~~Dissolved Fe(II) concentrations ~~to that~~mirrored the trend of $\delta^{13}C_{DIC}$ with a steep increase during the first 20 days followed by a decrease of 37 µM (Fig. 45).

3.1.5 Metabolic pathways

To ~~evaluate~~elucidate which metabolic processes drive AOM, we analyzed $\delta^{13}C_{DIC}$ following the addition of inhibitors to the second stage long-term slurries: i) BES, a specific inhibitor for ~~methanogens and ANME's *mcrA* genes~~methanogenesis (Nollet et al., 1997) and ii) acetylene, a non-specific inhibitor for ~~methanogens. Both~~methanogenesis and methanotrophy (Orembland and Capone, 1988). In both cases ~~showed complete inhibition of~~and similar to the killed control, labeled ^{13}C-DIC production was completely inhibited following the addition~~, similarly to the killed control~~ (Fig. 6). Though acetylene~~5).~~ ~~Acetylene~~ can also inhibit nitrogen cycling in some cases~~; however, this~~, it has been shown to result in the production of ethylene (Oremland and Capone, 1988). In our case, however, no ethylene was

detected, supporting the ~~inhibition~~conclusion that only ~~of methanogens'~~the methanogenesis activity was inhibited.

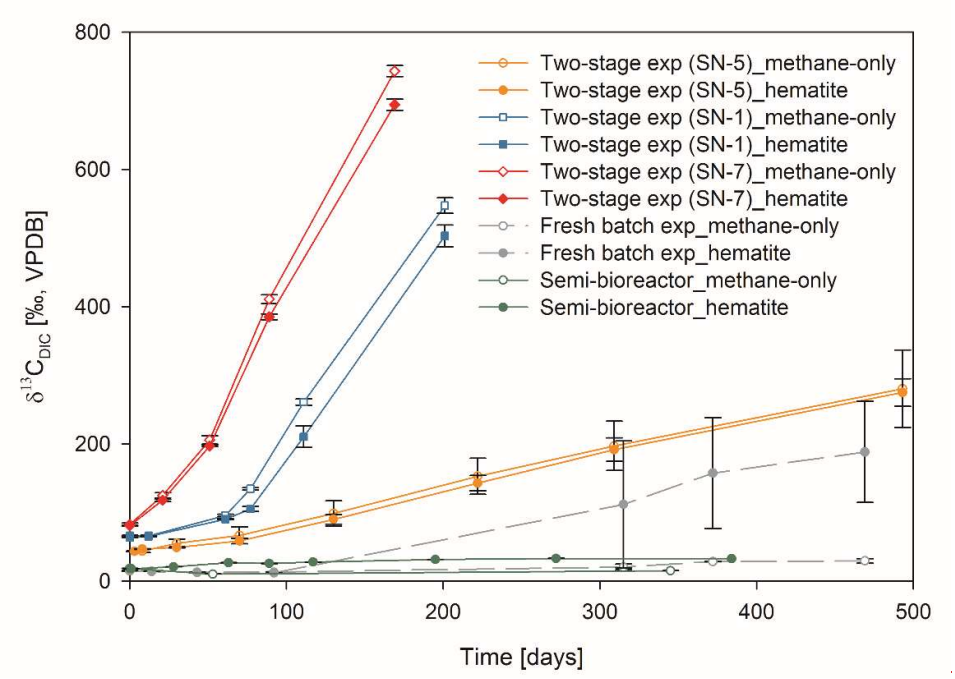

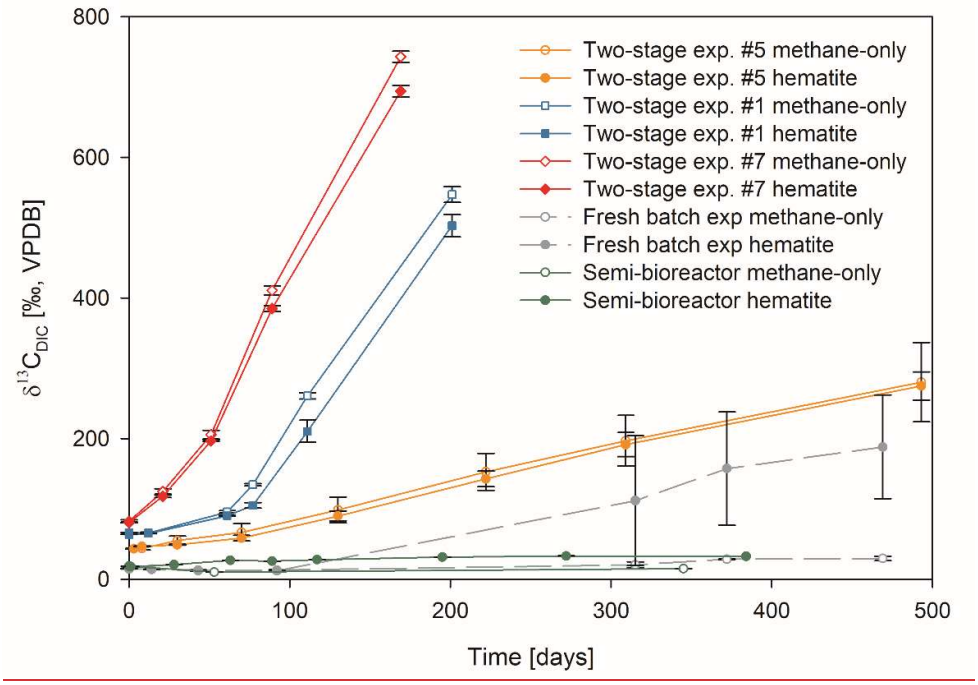

Figure ~~2~~3: Comparison of $\delta^{13}C_{DIC}$ values among the three types of experiments with ^{13}C -labeled methane addition: A) three two-stage slurry experiments~~;~~ (at the second stage of 1:3 ratio of sediment to porewater); B) the semi-continuous bioreactor experiment; and C) slurry batch experiment with freshly collected sediments (Bar-Or et al.,

2017). In each experiment, two treatments are shown, with hematite (filled symbol) and without hematite (empty symbols~~) hematite addition.~~). The error bars represent the average deviation of the mean of duplicate/triplicate bottles.

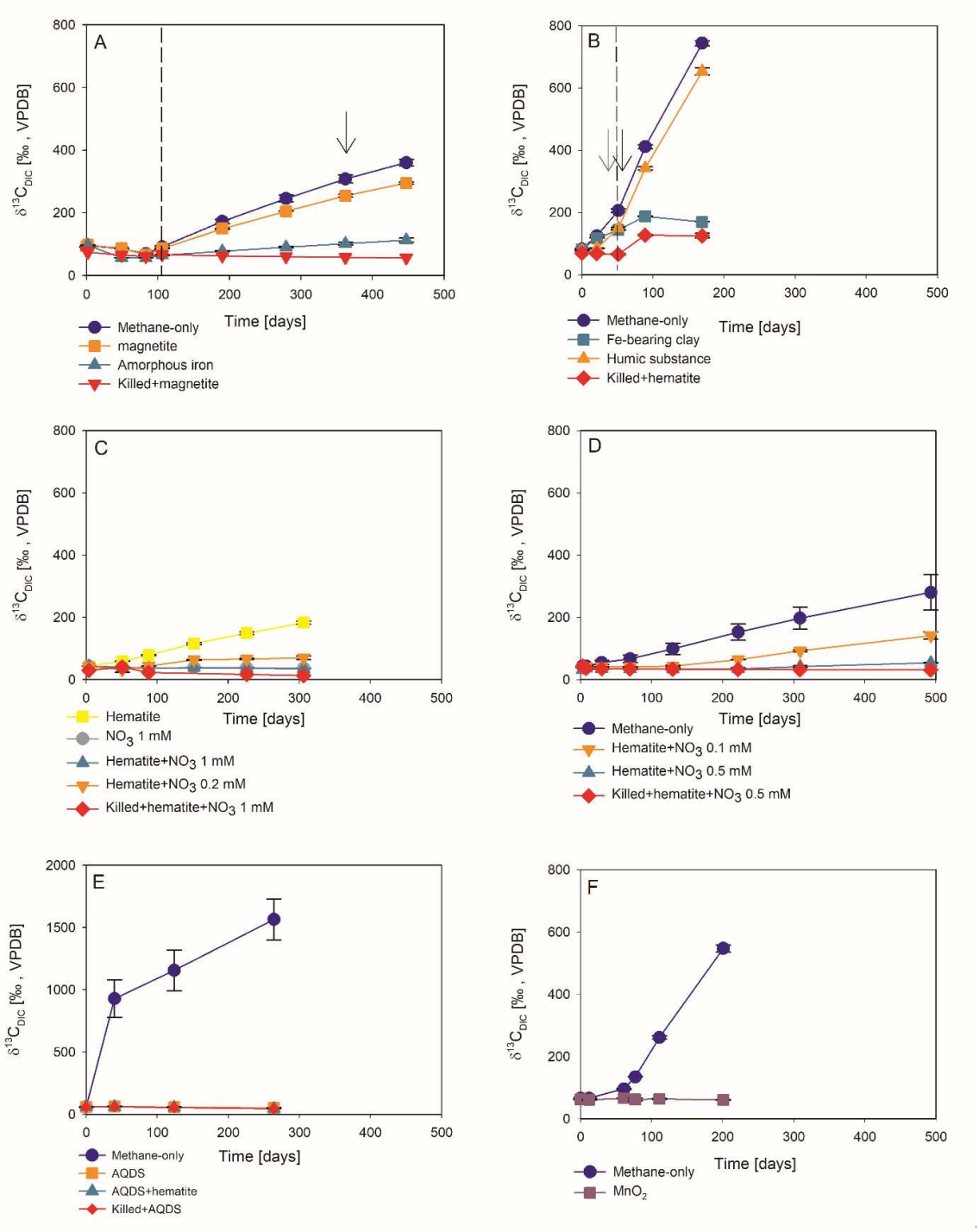
A
B
C
D
E
F
$\delta^{13}C_{DIC}$ [‰ , VPDB]
Time [days]
Methane-only
magnetite
Amorphous iron
Killed+magnetite
Methane-only
Fe-bearing clay
Humic substance
Killed+hematite
Hematite
NO_3 1 mM
Hematite+NO_3 1 mM
Hematite+NO_3 0.2 mM
Killed+hematite+NO_3 1 mM
Methane-only
Hematite+NO_3 0.1 mM
Hematite+NO_3 0.5 mM
Killed+hematite+NO_3 0.5 mM
Methane-only
AQDS
AQDS+hematite
Killed+AQDS
Methane-only
MnO_2

483

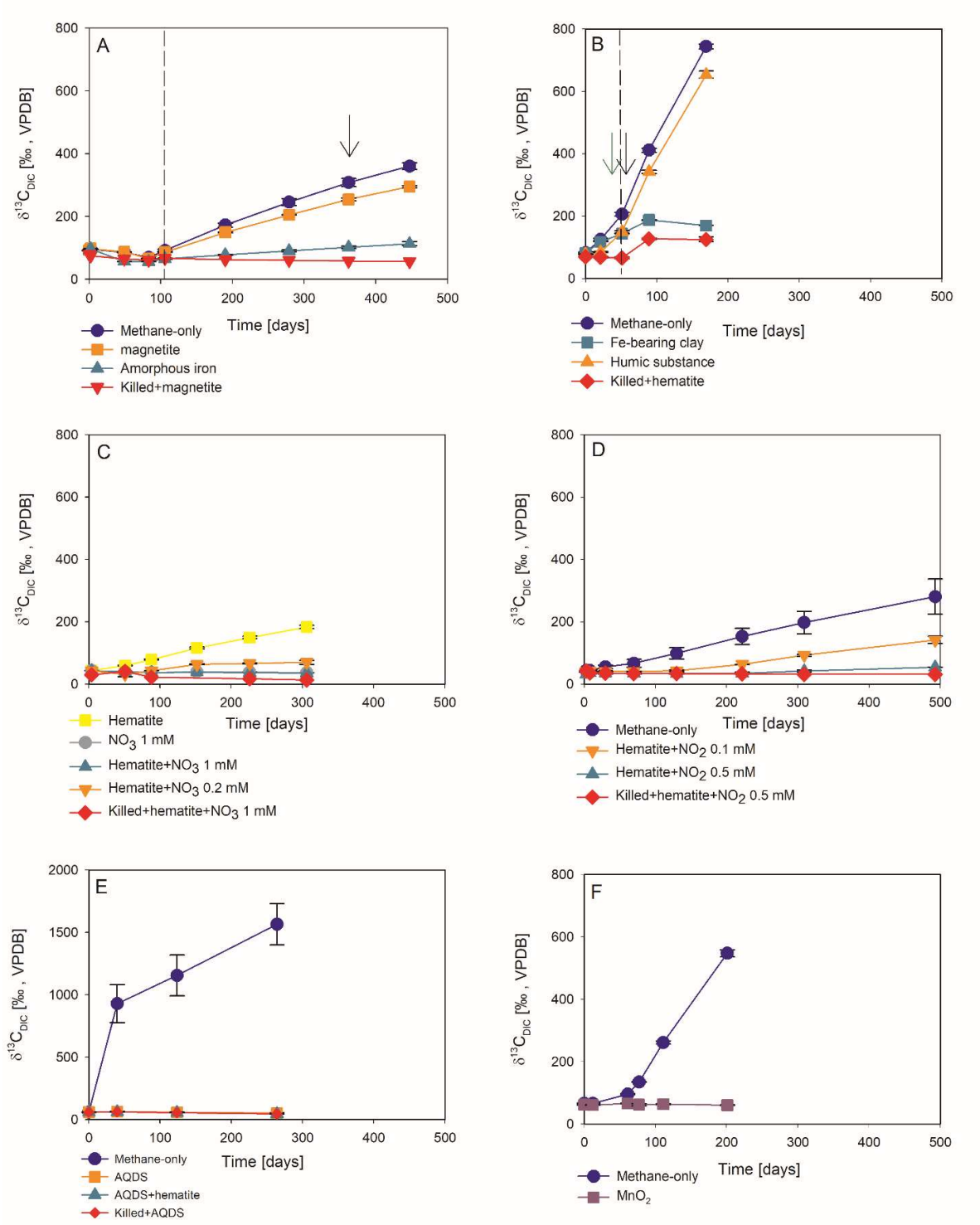

Figure ~~3: The potential~~4: Potentials of different electron acceptors for AOM in Lake Kinneret in the ~~pre-incubated~~two-stages long-term slurry experiments (at the second stage of 1:3 ratio of sediment to porewater) with of ^{13}C -labeled methane and the following treatments: (A) with and without the addition of magnetite and amorphous iron ($Fe(OH)_3$). The dashed line represents the ~~addition~~specific time of ^{13}C -labeled ~~CH_4~~methane addition. The black arrow represents the addition of Na-molybdate as an inhibitor for sulfate reduction. (B) with

clay and natural humic substance. The green arrow represents the time clay was added to the relevant bottles, the dashed line represents the time the headspace of ~~the bottles~~each bottle was flushed again with N_2, and the black arrow represents the second injection of 1 mL of ^{13}C-labeled methane. (C) with the addition of hematite and two different concentrations of nitrate. (D) with the addition of hematite and two different concentrations of nitrite. (E) with the addition of AQDS. (F) with and without the addition of ^{13}C-labeled methane ~~was added~~ to all of the bottles (see Table 1 for specific experimental details ~~on each experiment can be found in Table 1).~~). Error bars represent the average ~~of the absolute~~ deviations of the data points from their ~~mean~~means of duplicate/triplicate bottles.

Table 2: ~~Methanogenesis~~ AOM rates and AOM ~~rates~~role in experiment A ~~(two-~~second stage slurries~~)~~ amended with ^{13}C-labeled methane and different electron acceptors (assuming methanogenesis rate ~~was calculated in one of the experiments and was assumed to be similar in all of them~~24.8 nmol g DW^{-1} d^{-1}).

Experiment serial number (SN)	Treatment	Methanogenesis rate [nmol/gr dry sediment X day]	AOM rate [nmol/gr dry sediment X day]	AOM/methanogenesis [%]
10	**methane only**	24.8	1.1	4.4
1	**methane only**	24.8	1.6	6.4
	methane+hematite	24.8	0.5	2.1
2	**methane only**	24.8	2.4	8.2
	methane+magnetite	24.8	1.8	6.3
	methane+amorphous iron	24.8	0.1	0.5
7	**methane only**	24.8	1.4	6.4
	methane+hematite	24.8	1.3	6.0
	methane+humics	24.8	1.2	5.4
5	**methane only**	24.8	1.0	4.6
	methane+hematite	24.8	1.0	4.6
	methane+hematite+nitrite 0.5 mM	24.8	0.2	0.8
	methane+hematite+nitrite 0.1 mM	24.8	0.5	2.1

Experiment serial number (SN)	Treatment	AOM rate [nmol/g DW X d]	AOM/methanogenesis [%]
10	**methane only**	1.1	4.4
1	**methane only**	1.6	6.4
	methane+hematite	0.5	2.1
2	**methane only**	2.4	8.2
	methane+magnetite	1.8	6.3
	methane+amorphous iron	0.1	0.5
7	**methane only**	1.4	6.4
	methane+hematite	1.3	6.0
	methane+humics	1.2	5.4
5	**methane only**	1.0	4.6
	methane+hematite	1.0	4.6
	methane+hematite+nitrite 0.5 mM	0.2	0.8
	methane+hematite+nitrite 0.1 mM	0.5	2.1

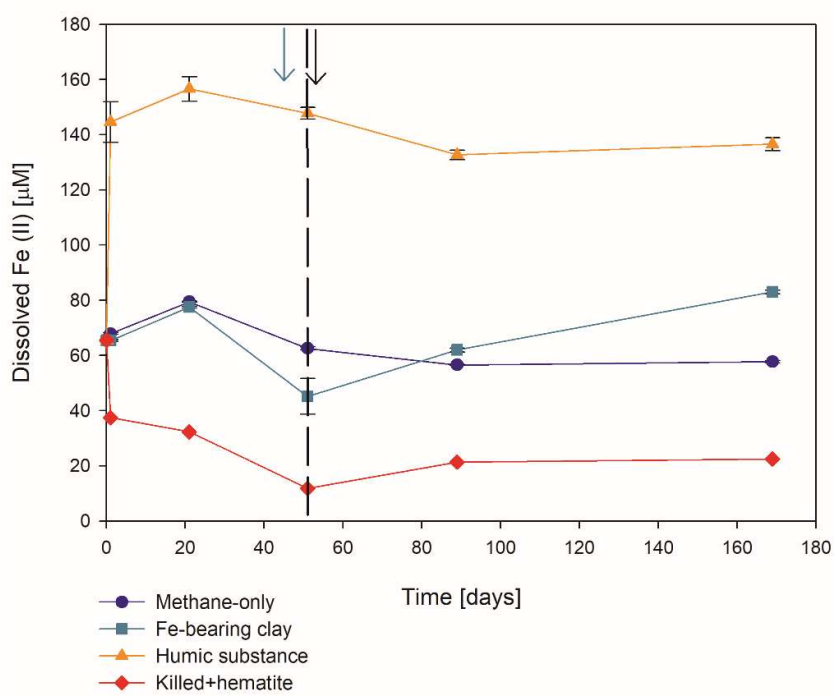

Figure 4: The5: Change in dissolved Fe(II) change in the two-second stage of experiment No. 7 containing clay, and natural humic acid, and PCA. The green arrow represents the time at which clay was added to the specific bottles and those bottles were flushed with N_2, the dashed line represents the time at which the rest of the bottles were flushed, and the black arrow represents the time $^{13}CH_4$at which ^{13}C-labeled methane was added again. Error bars represent the average of the absolute deviations of the data points from their meanmeans.

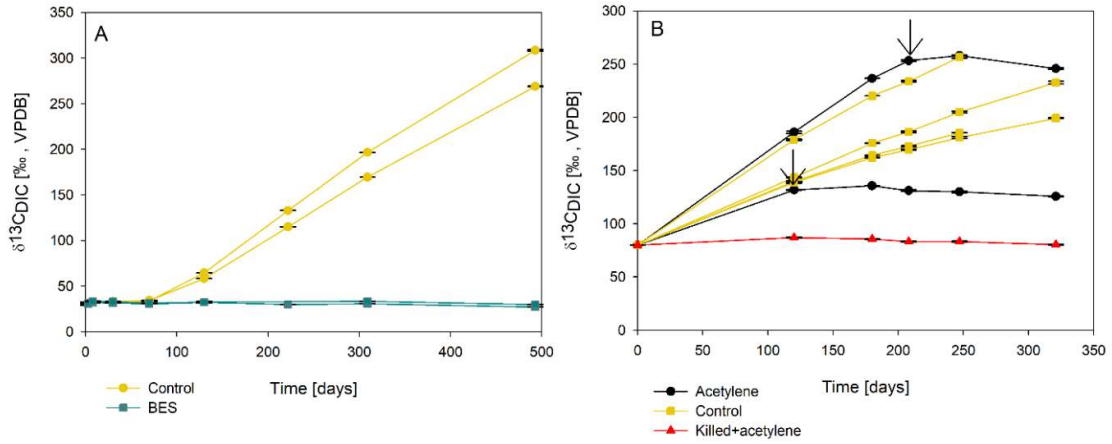

Figure 6: Change in $\delta^{13}C_{DIC}$ values over time in the second stage long-term sediment slurry incubations amended with hematite and ^{13}C-labeled methane. (A) with/without BES and (B) with/without acetylene. Black arrows represent the time at which acetylene was injected into the experiment bottle. The error bars are smaller than the symbols.

3.2 Microbial dynamics

Analyses of taxonomy and coverage of metagenome-assembled genomes suggest that in the pre-incubated two-stage slurries, Bathyarchaeia are the dominant archaea, together with putative methanogens such as Methanofastidiales (Thermococci), Methanoregulaceae (Methanomicrobia) and Methanotrichales (~~Methanosarcinia~~Methanosarcina) (Supplementary coverage table). ~~Bonafide~~Bona-fide ANME (ANME-1) were detected ~~at~~with substantial coverage of approximately 1 (the 27th most abundant ~~out of~~ from among the 195 MAGs detected) in all of the treatments. Among the bacteria, the sulfate reducers Desulfobacterota and Thermodesulfovibrionales (Nitrospirota) were prominent together with the GIF9 Dehalococcoida lineage, which is known to metabolize chlorinated compounds in lake sediments (Biderre-Petit et al., 2016). Some Methylomirabilales (NC10) were found (average coverage of 0.32±0.06), and no Methanoperedens were detected. Methylococcales methanotrophs were found in the natural sediments and the fresh batch and bioreactor incubations (average of 0.34±0.02), ~~as opposed~~in contrast to ~~the~~their average coverage of 0.09±0.04 in the long-term incubations. Methylococcales comprised the *Methyloterricola*, *Methylomonas* and *Methylobacter* genera (Supplementary coverage table). The methylotrophic partners of aerobic methanotrophs, *Methylotenera*, were found in fresh batch and bioreactor incubations, where *Methylomonas* was found, findings that are in line with those of previous studies ~~showing~~that showed their association (Beck et al., 2013). Principal component analysis shows the grouping of long-term, pre-incubated slurries, semi-aerobic bioreactor incubations, and fresh batch experiments (Fig. ~~6~~7), emphasizing the microbial dynamics over time.

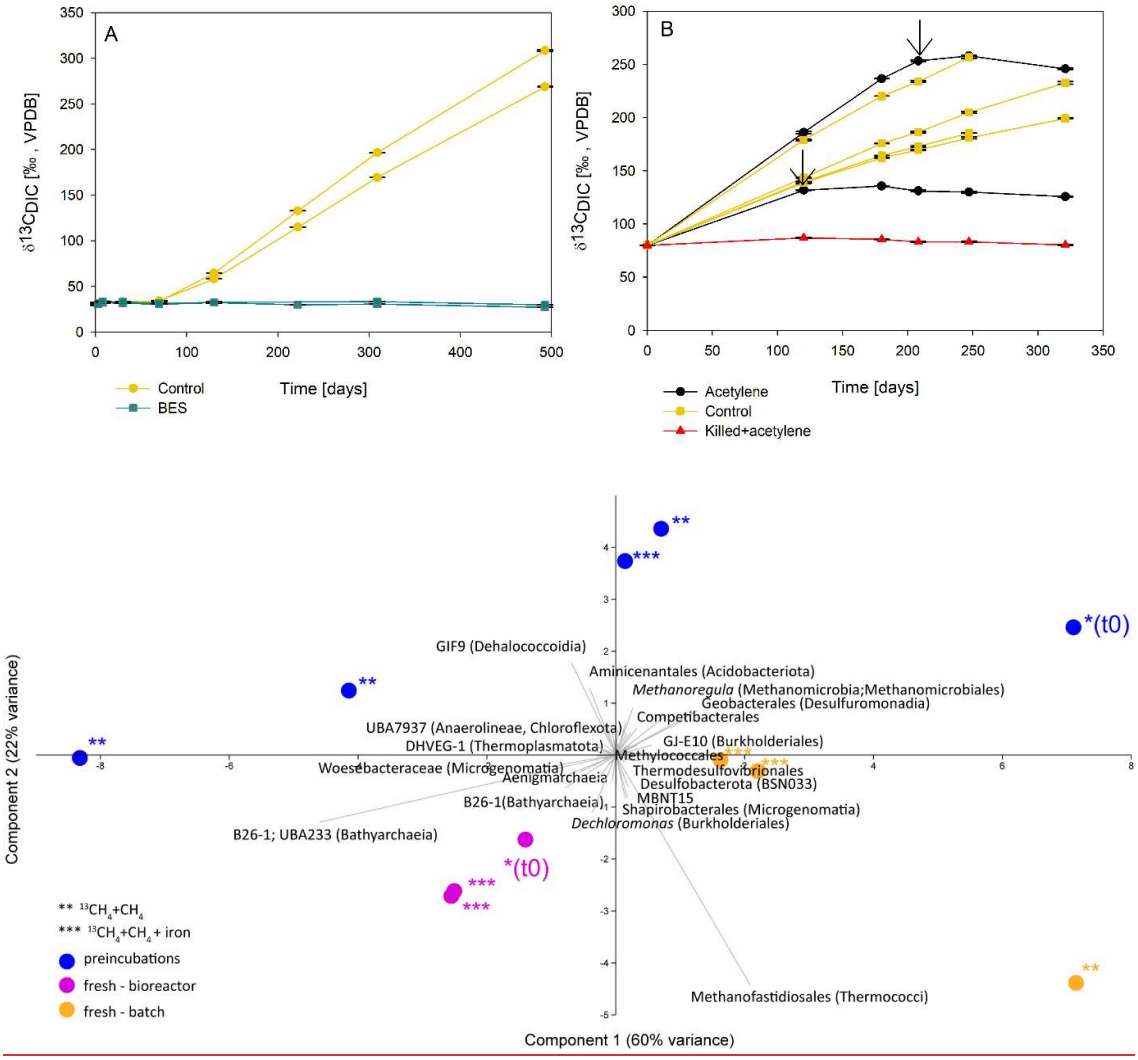

Figure ~~5: The change of $\delta^{13}C_{DIC}$ values with time in two long-term sediment slurry incubations amended with hematite and ^{13}C-labeled methane. (A) with/out BES and (B) with/out acetylene. Black arrows represent the time at which acetylene was injected to the experiment bottle. The error bars are smaller than the symbols.~~

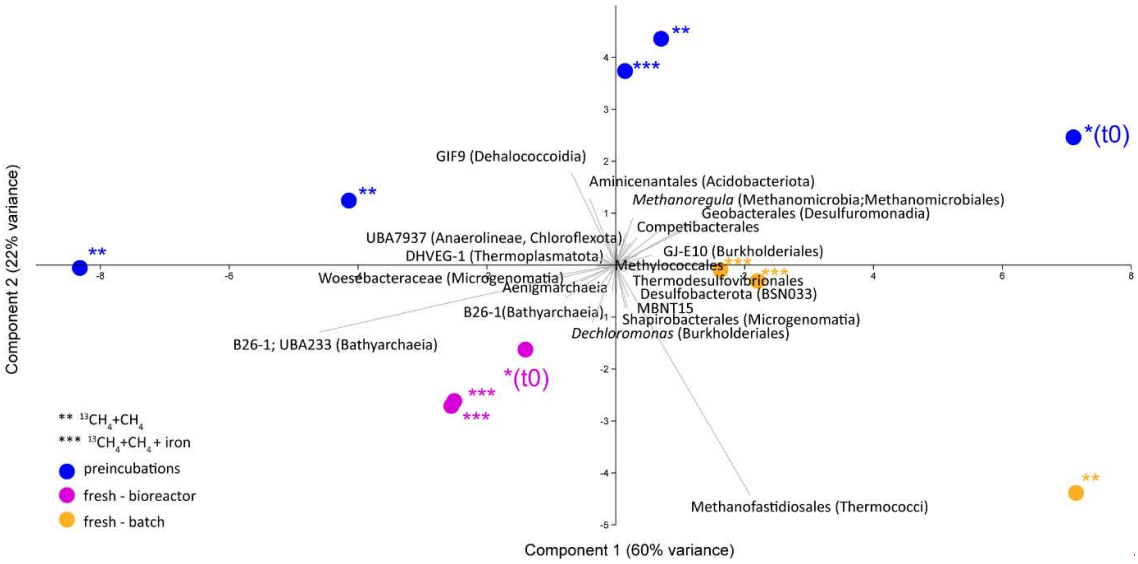

Figure ~~6~~7: Principal component analysis ~~comparing~~comparison of three types of samples: long-term pre-incubated slurries (blue – experiment A), semi-continuous bioreactor (pink – experiment B) and fresh batch experiments (orange – experiment C). One asterisk represents t0, two asterisks denote methane-only treatments, three asterisks represent hematite treatment.

3.3 Lipid analysis

The $\delta^{13}C$ values of the archaeol-derived isoprenoid phytane were between −5 and −17‰ in the long-term pre-incubated samples ~~were between -5 and -17‰~~ and thus showed ~~a~~ ^{13}C-enrichment ~~between~~of 15- to 27‰ relative to the original sediment~~,~~. This is indicative of methane-derived carbon assimilation by archaea (Table 3). ~~This was less pronounced for acyclic~~Acyclic biphytane, ~~dominantly~~ derived mainly from caldarchaeol, ~~which showed a~~ exhibited a less pronounced ^{13}C-enrichment of 5-10‰. For bacterial-derived fatty acids, ~~the shift in~~ $\delta^{13}C$-values ~~of~~similarly shifted by up to 10‰ relative to the original sediment ~~was in a similar range but~~. Nonetheless, one would have ~~been~~ expected values to be ~~much~~extremely higher if aerobic methanotrophs were active, as was previously indicated by ~~the extreme~~strong ^{13}C-~~enrichment~~enrichments of up to 1,650‰ in $C_{16:1\omega5c}$ observed in freshly incubated batch samples (Bar-Or et al., 2017).

Table 3: The $\delta^{13}C$ values (in ‰) of fatty acids and isoprenoid hydrocarbons from different experiments compared to values obtained from the original sediment in the methanogenic zone.

			Fatty acids		Hydrocarbons	
Description	Temperature (°C)	Sampling (days)	$C_{16:1\omega9/8/7}$	$C_{16:1\omega5}$	Phytane	Biphytane
Pre-incubated slurry +$^{13}CH_4$+hematite	20	411	-40	-43	-17	-23
Pre-incubated slurry +$^{13}CH_4$ (bottle A)	20	411	-40	-43	-13	-24
Pre-incubated slurry +$^{13}CH_4$ (bottle B)	20	1227	-36	-41	-5	-38
[a] Fresh batch experiment+$^{13}CH_4$+hematite	20	470	610	1600	-14	-28
Semi-bioreactor+$^{13}CH_4$+hematite	16	382	n.d.	n.d.	n.d.	n.d.
Original sediment (28-30 cm)	14		-44	-51	-32	-33

[a] Bar-Or et al., 2017
n.d. – Not detected

4. Discussion

4.1 ~~AOM is maintained~~Anaerobic oxidation of methane in ~~long-term two-stage~~the methanogenic sediment incubation experiments

~~Our previous porewater profiles of Lake Kinneret indicate that microbial sulfate reduction dominates the anoxic hypolimnion and the surface sediments, while methanogenesis is confined to the sediments below the sulfate boundary (Adler et al., 2011; Sivan et al., 2011; Bar-Or et al., 2015).~~ The *in-situ* geochemical and microbial diversity profiles~~, as well as~~ (Bar-Or et al., 2015) and the geochemical (Sivan et al., 2011; Bar-Or et al., 2017; Fig. 3) and metagenomic (Elul et al., 2021) analyses of batch incubations with fresh sediments~~,~~ provided ~~evidence~~strong support for the occurrence of Fe-AOM in sediments of the ~~deep~~ methanogenic zone below 20 cm ~~depth (Adler et al.,~~. Such ~~2011; Sivan et al., 2011; Bar-Or et al., 2015; Bar-Or et al., 2017; Elul et al., 2021; Fig. 2). The~~ profiles and ~~the~~alongside incubations showed an unexpected presence of aerobic bacterial methanotrophs together with anaerobic microorganisms, such as methanogens and iron reducers (Adler et al., 2011; Sivan et al., 2011; Bar-Or et al., 2015; Bar-Or et al., 2017; Elul et al., 2021~~, in the anoxic sediments. They~~). These findings suggested that both *mcr* gene-bearing archaea and aerobic bacterial methanotrophs mediate methane oxidation. In ~~this~~the current study ~~analyses~~, we have supportive evidence of ~~^{13}C-DIC derived from ^{13}C-labeled methane suggest that~~ considerable AOM ~~takes place also~~ in the long-term incubations, even after the two treatment stages and considering the low abundance of the microbial populations. ~~Below, we characterize this AOM process in these incubation experiments.~~

~~4.1 Potential electron acceptors for AOM in the long-term two-stage incubation experiments~~

The ~~pre-incubated long-term incubations~~ data ~~show a sharp increase~~from the second stage incubations show a similar increasing trend in the $\delta^{13}C_{DIC}$ values of both natural (methane-only) and the hematite ~~amendments in the two-stage incubations (Fig. 2). However, no difference in $\delta^{13}C_{DIC}$ between the two~~amended treatments ~~was observed following the addition of hematite as the electron acceptor.~~(Fig. 3). This ~~differs~~deviates from ~~the~~our observations during experiments B and C ~~observations~~ with fresh

sediment, ~~where the addition of hematite showed~~wherein higher $\delta^{13}C_{DIC}$ values were obtained after the addition of hematite than in the methane-only treatment (Fig. ~~2;~~3 and Bar-Or et al~~.~~, (2017~~).~~)). This was particularly dramatic in the batch slurries (experiment C), but it was also ~~significant~~observed in the semi-continuous bioreactor (experiment B). We ~~believe~~assume that the observed difference in the bioreactors would have been more pronounced if methane concentrations ~~were~~had been higher, but it is still ~~significant.~~a significant finding. We also note that the difference between the bioreactors results may also be due to the fact that each bioreactor community developed separately. The results of the type A experiments (compared to those of types B and C) suggest that either hematite lacks the potential to stimulate the AOM activity during ~~long-term~~ the two-stage experiments or ~~the presence of~~that there is enough natural Fe(III) in the sediments to sustain the maximum potential of Fe-AOM. Below we characterize the AOM process in the long-term, two-stage incubation experiments.

4.2 Potential electron acceptors for AOM in the long-term two-stage incubation experiments

Measurements of $\delta^{13}C_{DIC}$ show that the additions of magnetite, amorphous iron, ~~ferric iron from~~ clays and manganese oxide in the ~~two-~~second stage incubations ~~result~~resulted in a less pronounced increase in the $\delta^{13}C_{DIC}$ values compared to those of the methane-only controls (~~Figs. 2 and 3), reducing the AOM signal. One~~Fig. 4). A possible explanation ~~is~~for the latter may be that these metal oxides ~~may~~ inhibit AOM, either directly or ~~by~~via a preference for organoclastic iron reduction over Fe-AOM, which adds ~~isotopically light~~a natural, more negative carbon isotope signal from the ~~organics~~organic materials rather than the heavy carbon from the ^{13}C-labeled methane. Using mass-balance estimations in the methane-only ~~treatments~~ and in the amorphous iron ~~ones~~treatments and considering the DIC concentrations and $\delta^{13}C_{DIC}$ values of the methane-only treatments at the beginning of the experiment (6~~-~~ mM and 60‰, respectively) and the values at the end (6.5 mM and 360‰, respectively), about 0.5~~-~~ mM of the DIC was added by the AOM of methane with $\delta^{13}C$ of ~4000‰. The DIC and $\delta^{13}C_{DIC}$ values of the amorphous iron treatment at the beginning of the experiment were 5.4 mM and 60‰, respectively, and ~~the values at~~by the end were 6.1 mM and 120‰, respectively. Assuming the same $\delta^{13}C$ of the added methane of 4000‰ and a $\delta^{13}C_{TOC}$ of ~~-~~-30‰ (Sivan et al., 2011), 0.1 mM of the DIC should derive from AOM and 0.6 mM from organoclastic metabolism. This means that adding amorphous iron to the system ~~decreased the AOM activity and~~ encouraged iron reduction that was coupled to the oxidation of ~~other~~ organic compounds ~~rather~~other than methane. Intrinsic microbes, particularly the commonly detected ex-deltaproteobacterial lineages such as Geobacterales, may catalyze Fe(III) metal reduction, regardless of AOM~~.~~ (Xu et al., 2021). Manganese oxides are found in very low abundance in Lake Kinneret sediments (0.1 %, Table S1 and Sivan et al., 2011). Thus, their role in metal-AOM is likely minimal.

Sulfate concentrations in the methanogenic Lake Kinneret sediments ~~are low (<~~ have been below the detection limit in years past, similar to their representation in the natural sediments we used for the

incubations (< 5 µM, Bar-Or et al., 2015; Elul et al., 2021). Sulfide concentrations have also been reported to be minor (< 0.3 µM, Sivan et al., 2011). However, ~~since~~sulfate could theoretically still be a short-lived intermediate for the AOM process, as pyrite and FeS precipitate in the top sediments, and cryptic cycling via pyrite or FeS may replenish the sulfate, thus rendering it available for AOM (Bottrell et al., 2000). The addition of Na-molybdate ~~addition~~ to the ~~two~~ second stage slurries, including those amended with and without magnetite, did not change the $\delta^{13}C_{DIC}$ dynamics, which remained similar to those from before the ~~inhibitor's~~ addition of the inhibitor (Fig. ~~3A~~4A). This finding is in line with ~~the~~that in fresh batch sediment slurries (Bar-Or et al., 2017) and ~~hints~~suggests that sulfate is not a potent electron acceptor for AOM in this environment. Furthermore, although sulfate-reducing bacteria were abundant, none of ~~these~~the reducers belonged to the known clades of ANME-2d partners ~~(Supplementary coverage table~~, which were connected previously to the Fe-S-CH_4 coupled AOM (Su et al., 2020; Mostovaya et al., 2021).

~~The nitrate~~Nitrate and nitrite concentrations are also undetectable in the porewater of Lake Kinneret sediments (Nüsslein et al., 2001; Sivan et al., 2011), but ~~they~~again may ~~occur~~appear as ~~an~~short-lived intermediate ~~product~~products of ammonium oxidation that is coupled to iron reduction~~.~~ (Tan et al., 2021; Ding et al., 2014; Shrestha et al., 2009; Clement et al., 2005). We thus assessed the ~~role~~roles of nitrate and nitrite as electron acceptors in the two-stage slurries. ~~The~~Our results indicate that the addition of nitrate ~~delayed~~did not promote AOM ~~and~~, likely ~~promoted denitrification. This is consistent with~~due to the ~~fact that~~absence of ANME-2d ~~was not found.~~, which is known to use nitrate (Arshad et al., 2015; Haroon et al., 2013). In the case of nitrite, even low concentrations appeared to delay the increase in $\delta^{13}C_{DIC}$ values, suggesting that organoclastic denitrification outcompetes AOM, and despite the occurrence of Methylomirabilia, the role of nitrite-AOM is not prominent in the two-stage incubations~~,~~ ~~despite the occurrence of Methylomirabilia~~ (Figs. ~~3C~~4C, D).

Humic substances may promote AOM by continuously shuttling electrons to metal oxides (Valenzuela et al., 2019). ~~Humic~~Though humic substances were not measured directly in Lake Kinneret sediments, ~~but~~ the DOC concentrations in ~~porewater at~~ the methanogenic depth ~~were~~porewater were previously found to be high (~1.5 mM, Adler et al., 2011), suggesting that they may play a role in AOM. ~~The addition of~~ Compared to the methane-only treatments, the treatment with the synthetic humic ~~analogs~~analog AQDS ~~did not cause any enrichment in ^{13}C-DIC, but~~caused an increase ~~of the~~in dissolved Fe(II) concentrations ~~compared to the methane-only treatments.~~, but it did not cause ^{13}C-DIC enrichment. This may be explained by the behavior of AQDS ~~acting~~ as ~~an~~a strong electron shuttle in organoclastic iron reduction~~, producing~~ (Lovely et al., 1996), which produces isotopically ~~light~~more negative carbon that masks the AOM signal (Fig. ~~3E~~4E, Fig. ~~S4).~~ S3). Yet, as was done by Valenzuela et al. (2017), the addition of natural humic substances ~~may~~did promote AOM, compared to the rest of the electron acceptors tested, and may thus support AOM~~, as was suggested by Valenzuela et al. (2017).~~ (Fig. 4B). In our incubations, the natural humic substances promoted first the oxidation of organic

matter ~~and~~by iron reduction ~~at first~~, probably by shuttling electrons from the broad spectrum of organic compounds ~~other than methane~~ to natural iron oxides ~~in the sediments~~ (Figs. ~~3B~~4B and ~~4). Then, when~~5). When the availability of the iron oxides or the organic matter decreased, humic substances likely ~~facilitated~~took over to facilitate the AOM (Fig. ~~3B~~4B).

Overall, the results of our long-term ~~batch~~two-stage experiments~~, which included different electron acceptors,~~ indicate that sulfate, nitrate, nitrite and ~~Mn~~ manganese oxides do not support AOM in ~~Lake Kinneret~~ the methanogenic sediments~~.~~ of Lake Kinneret. The ~~potential~~candidate electron acceptors for AOM in the long-term experiments are natural humic ~~substrates with or without~~ substances and/or the naturally abundant iron minerals ~~that are abundant in the sediment and preferably react with methane rather than with other organics. The~~. Future experiments can simulate iron limitation and the involvement of iron oxides in the AOM ~~will be further explored after~~by removing natural iron oxides from the sediments ~~to simulate iron limitation.~~ .

4.~~2~~3 Main microbial players in the long-term ~~pre-incubated~~two-stage incubations

Methane oxidation in the pre-incubated Lake Kinneret sediments is likely mediated by either ANMEs or methanogens, as the addition of BES~~, a specific inhibitor for methanogens and ANME's mcrA genes,~~ and acetylene immediately stopped the AOM~~, similarly~~ (Fig. 6) similar to the results of the killed bottles~~,~~ and the BES ~~addition to~~treatment in the fresh ~~sediment experiments~~batch experiment (Bar-Or et a., 2017~~) (Fig. 5~~). Apart from methane-metabolizing ~~organisms~~, acetylene can inhibit nitrogen cycling, ~~resulting~~which results in ethylene production (Oremland and Capone, 1988). This ~~is~~was not the case in our incubations, as no ethylene was produced. The increase in $\delta^{13}C$ values in phytane and biphytane (Table 3) also indicates the presence of active archaeal methanogens or ANMEs (Wegener et al., 2008; Kellermann et al., 2012; Kurth et al., 2019).

Using the isotopic ~~composition~~compositions of specific lipids and metagenomics, we identified a considerable abundance of aerobic methanotrophs and methylotrophs in the fresh sediments, but not in the ~~pre-incubation~~long-term slurries (Table 3, Fig. ~~6), suggesting~~7). In the natural sediments, micro levels (nano molar) of oxygen could be trapped in clays and slowly released to the porewater (Wang et al., 2018). However, if such micro levels of oxygen still existed during the time of the pre-incubation, they were probably already exhausted. Indeed, the results of our specific lipids and metagenomics analyses suggest that the aerobic methanotrophs lineages play only a minor role ~~of these lineages in the latter.~~in the long-term slurries, probably due to complete depletion of the oxygen. The metagenomic data (Fig. ~~6~~7, Supplementary coverage table) also indicate that Bathyarchaeia, which ~~might~~may be involved in methane metabolism (Evens et al., 2015), were enriched in the bioreactor incubations, yet their role in Lake ~~Kineret~~Kinneret AOM remains to be evaluated. ~~ANME-1 are likely mediators of AOM in these sediments, although methane oxidation via the reverse methanogenesis is feasible for some methanogens in Lake Kinneret sediments (Elul et al., 2021).~~ We also observed changes in the

abundance of bacterial degraders of organic matter and necromass: for example, GIF9 Dehalococcoidia, which can metabolize complex ~~organies~~organic materials under methanogenic conditions (Cheng et al., 2019; Hug et al., 2013), were most abundant in the long-term incubations (Fig. ~~6~~7, Supplementary coverage table). Though ANME-1 are likely mediators of AOM in these sediments, methane oxidation via reverse methanogenesis is feasible for some methanogens in Lake Kinneret sediments (Elul et al., 2021).

4.~~3~~4 Mechanism of methane oxidation in the long-term two-stage incubations ~~– AOM versus back flux~~

Our results indicate net methanogenesis in the two-stage incubation experiments with an average rate of 25 nmol gr^{-1} dry sediment day^{-1} (~~Table 2,~~ Fig. ~~S3~~1 and Table S2), which are similar to those from fresh incubation experiments (Bar-Or et al., 2017~~),~~). This is despite the overall trend of increasing ~~trend of~~ $\delta^{13}C_{DIC}$ values ~~resulting from~~ , a result representing potential methane turnover (Figs. 2~~3~~ and ~~3~~4). A likely explanation for the presence of both signals is an interplay between methane production and oxidation, ~~with the latter~~which is possibly triggered by ~~reverse~~reversal of the methanogenesis pathway in ~~bona fide~~bonafide ANMEs or ~~some~~certain methanogens (Hallam et al., 2004; Timmers et al., 2017). Due to the overall production of methane and the lack of ~~intensive~~intense stimulation of AOM by any electron acceptor added, the ~~significant~~ increase in $\delta^{13}C_{DIC}$ values could theoretically result from the occurrence of carbon back flux during methanogenesis, which is feasible in environments that are close to thermodynamic equilibrium (Gropp et al., 2021). ~~We~~To test this, we used DIC mass balance calculations to determine ~~whether~~ the strength of back flux ~~can be accounted for~~ in ~~the~~our incubations. Based on equations 1 and 2, ~~3-~~the observed level of ^{13}C-enrichment indicates that 3-8% of the ^{13}C-methane should be converted into DIC ~~to reach the observed ^{13}C-enrichment.~~. These estimates are orders of magnitude higher than the previously reported values of 0.001-0.3% ~~values~~ for methanogenesis back flux in cultures (Zehnder and Brock, 1979; Moran et al., 2005), ~~and~~but they are in the same range as the back flux of 3.2 to 5.5% ~~of back flux~~ observed in ANME-enrichment cultures (Holler et al., 2011). ~~In contrast~~For the latter, however, modeling approaches from AOM-dominated marine sediment samples and associated ANME enrichment cultures indicated the absence of net methanogenesis (Yoshinaga et al., 2014; Chuang et al., 2019; Meister et al., 2019; Wegener et al., 2021). Thus, it ~~is~~seems unlikely that back flux alone can account for the methane-to-DIC conversion in Lake Kinneret sediments. Moreover, ~~just~~the occurrence of back flux alone in marine methanogenic ~~sediment~~sediments with similar net methanogenesis rates and abundant methane-metabolizing archaea did not yield ~~any significant~~considerable ^{13}C-enrichment in the DIC pool following sediment incubations (Sela-Adler et al., 2015; Amiel, 2018; Vigderovich et al., 2019; ~~Yorshensky~~Yorshansky, 2019) (Table S3). ~~Therefore, methanogenesis back flux alone seems~~It is, therefore, less likely ~~to sustain~~that the observed DIC values in our study were sustained by methanogenesis back flux alone

(without an external electron acceptor) than by active AOM~~.~~, which, in this case, is probably performed by ANME-1 or by methanogens that perform reverse methanogenesis to some extent.

Conclusions

~~The geochemical and microbial profiles together with fresh sediment incubations showed evidence for Fe-AOM in the methanogenic zone of Lake Kinneret, which removes about 10-15% of the produced methane (Adler et al., 2011; Sivan et al., 2011). Anaerobic archaea appear to carry out methane turnover in these reduced sediments by reverse methanogenesis, but aerobic Methylococcales may be involved in methane oxidation, which is in line with other evidence of aerobic bacterial activity in the deep anoxic hypolimnion of lakes and their shallow sediments (Beck et al., 2013; Oswald et al., 2016; Martinez-Cruz et al., 2017; Cabrol et al., 2020). The simultaneous presence of aerobes and anaerobes in nature, even 20 meters below the thermocline and oxycline, may result from trace amounts of oxygen trapped in nano-niches or even in mineral layers (Wang et al., 2018), even if sensitive sensors do not detect them. This oxygen portion may not be removed by purging at the beginning of our experiments but is rather slowly used by the methanotrophs for their survival. However, after several incubation stages and intensive purging for a prolonged time, only archaea remained active and were involved in methane turnover, which was most likely coupled to the reduction of electron acceptors such as humic substances and iron.~~

The previous results of the geochemical and microbial profiles and the fresh sediment incubations from Lake Kinneret sediment constitute evidence of the occurrence of Fe-AOM, which removes about 10-15% of the methane produced in the lake's sediment (Adler et al., 2011; Sivan et al., 2011). Anaerobic archaea appear to be responsible for the methane turnover in these reduced sediments by reverse methanogenesis, but aerobic Methylococcales may oxidize methane in these sediments as well. The co-occurrence of aerobes and anaerobes in the natural environment may be the result of the presence of undetected trace amounts of oxygen that are trapped at those depths in "nano-niches" or even in mineral layers (Wang et al., 2018). This oxygen portion may not be removed by purging at the beginning of our experiments but is rather slowly used by the methanotrophs for their survival. However, after two incubation stages and intensive purging for a prolonged duration, only archaea remained active and were involved in the observed methane turnover, consuming 3-8% of the methane produced. Thus, we propose two modes of methanotrophy in Lake Kinneret sediments: i) methane oxidation performed by Methylococcales species. This mode was observed only in the incubations with freshly collected sediments (batch or bioreactor). ii) methane oxidation through reverse methanogenesis performed most likely by ANME-1 or specific methanogens. This mode was observed in all incubation types and could be a result of carbon back flux, however, the very high $\delta^{13}C_{DIC}$ signal points to a metabolic reaction. This AOM is most probably coupled to the reduction of iron and/or humic substances, as terminal electron acceptors or as electron shuttles stimulating the Fe-AOM.

Competing interests. The authors declare that they have no conflict of interest.

~~**Acknowledgements**~~

Acknowledgments

We would like to thank B. Sulimani and O. Tzabari from the Yigal Allon Kinneret Limnological Laboratory for their onboard technical assistance. We thank all of O. Sivan's lab members for their help during sampling~~,~~ and especially heartfelt thanks to N. Lotem for the ~~help~~invaluable assistance with the mass balance calculations and the fruitful discussions and to E. Eliani-Russak for her technical assistance. Many thanks to K. Hachmann from M. Elvert's lab for his help during lipid analysis and to J. Gropp for insightful discussions ~~on~~about the back flux. This work was supported by ~~the~~ ERC consolidator ~~grant~~ (818450) and ~~the~~ Israel Science Foundation (857-2016) ~~of~~ grants awarded to O. Sivan. Funding for M. Elvert was provided by the Deutsche Forschungsgemeinschaft (DFG) ~~(~~under Germany's Excellence Initiative/Strategy through the Clusters of Excellence EXC 309 'The Ocean in the Earth System' (project no. 49926684) and EXC 2077 ~~(~~'The Ocean Floor—Earth's Uncharted Interface' (project no. 390741601). Funding for M. Rubin-Blum was provided by the Israel Science Foundation (913/19), the U.S.-Israel Binational Science Foundation (2019055) and the Israel Ministry of Science and Technology (1126~~), and~~). H. Vigderovich was supported by ~~the~~a student fellowship ~~of~~from the ~~Israeli water authority~~Israel Water Authority.

References

Adler, Michal, Eckert, W., & Sivan, O. (2011). Quantifying rates of methanogenesis and methanotrophy in Lake Kinneret sediments (Israel) using porewater profiles. *Limnology and Oceanography*, *56*(4), 1525–1535. https://doi.org/10.4319/lo.2011.56.4.1525

Aepfler, R. F., Bühring, S. I., & Elvert, M. (2019). Substrate characteristic bacterial fatty acid production based on amino acid assimilation and transformation in marine sediments. *FEMS Microbiology Ecology*, *95*(10), 1–15. https://doi.org/10.1093/femsec/fiz131

Amiel, N. (2018). *Authigenic magnetite in deep sediments.* MsC thesis, Ben Gurion University of the Negev.

~~Aromokeye, D. A., Kulkarni, A. C., Elvert, M., Wegener, G., Henkel, S., Coffinet, S., Eickhorst,T., Oni, O. E., Richter-Heitmann, T., Schnakenberg, A., Taubner, H., Wunder, L., Yin, X., Zhu, Q., Hinrichs, KU., Kasten, S., & Friedrich, M. W. (2020). Rates and Microbial Players of Iron-Driven Anaerobic Oxidation of Methane in Methanic Marine Sediments. *Frontiers in Microbiology*, *10*(January), 1–19. https://doi.org/10.3389/fmicb.2019.03041~~

Arshad, A., Speth, D. R., De Graaf, R. M., Op den Camp, H. J. M., Jetten, M. S. M., & Welte, C. U. (2015). A metagenomics-based metabolic model of nitrate-dependent anaerobic oxidation of methane by Methanoperedens-like archaea. *Frontiers in Microbiology*, *6*(DEC), 1–14. https://doi.org/10.3389/fmicb.2015.01423

Bai, Y. N., Wang, X. N., Wu, J., Lu, Y. Z., Fu, L., Zhang, F., Lau, TC., & Zeng, R. J. (2019). Humic substances as electron acceptors for anaerobic oxidation of methane driven by ANME-2d. *Water Research*, *164*, 114935. https://doi.org/10.1016/j.watres.2019.114935

Bankevich, A., Nurk, S., Antipov, D., Gurevich, A. a., Dvorkin, M., Kulikov, A. S., Lesin, V. M., Nicolenko, S. I., Pham, S., Prjibelski, A. D., Sirotkin, A. V., Vyahhi, N., Tesler, G., Aleksyev, A. M., & Pevzner, P. a. (2012). SPAdes: A New Genome Assembly Algorithm and Its Applications to Single-Cell Sequencing. *Journal of Computational Biology*, *19*(5), 455–477. https://doi.org/10.1089/cmb.2012.0021

Bar-Or, I., Ben-Dov, E., Kushmaro, A., Eckert, W., & Sivan, O. (2015). *Methane-related changes in prokaryotes along geochemical profiles in sediments of Lake Kinneret (Israel) Methane-related changes in prokaryotes along geochemical profiles in sediments of Lake Kinneret (Israel)*. (August). https://doi.org/10.5194/bg-12-2847-2015

Bar-Or, I., Elvert, M., Eckert, W., Kushmaro, A., Vigderovich, H., Zhu, Q., Ben-Dov, E., & Sivan, O. (2017). Iron-Coupled Anaerobic Oxidation of Methane Performed by a Mixed Bacterial-Archaeal Community Based on Poorly Reactive Minerals. *Environmental Science & Technology*, *51*, 12293–12301. https://doi.org/10.1021/acs.est.7b03126

~~Beal, E. J., House, C. H., & Orphan, V. J.~~Bastviken D. (2009). ~~Manganese-and Iron-Dependent Marine~~ Methane ~~Oxidation. *Science (New York, N.Y.)*, *325*(5937), 184–187. https~~. In: Likens G.E., ed. Encyclopedia of Inland waters, Oxford: Elsevier, 783–805.

http://doi.org/10.1126/science.1169984 1016/B978-012370626-3.00117-4.

Beck, D. A. C., Kalyuzhnaya, M. G., Malfatti, S., Tringe, S. G., del Rio, T. G., Ivanova, N., Lidstorm, M. E., & Chistoserdova, L. (2013). A metagenomic insight into freshwater methane-utilizing communities and evidence for cooperation between the Methylococcaceae and the Methylophilaceae. *PeerJ*, *2013*(1), 1–23. https://doi.org/10.7717/peerj.23

Biderre-Petit, C., Dugat-Bony, E., Mege, M., Parisot, N., Adrian, L., Moné, A., Denonfoux, J., Peyretaillade, E., Debroas. D., Boucher, D., Peyret, P. (2016). Distribution of Dehalococcoidia in the anaerobic deep water of a remote meromictic crater lake and detection of Dehalococcoidia-derived reductive dehalogenase homologous genes. *PLoS ONE*, *11*(1), 1–19. https://doi.org/10.1371/journal.pone.0145558

Boetius, A., Ravenschlag, K., Schubert, C. J., Rickert, D., Widdel, F., Gieseke, A., Amann, R., Jørgensen, B.B., Witte, U., & Pfannkuche, O. (2000). A marine microbial consortium apparently mediating AOM. *Nature*, *407*(October), 623–626.

Bottrell, S. H., Parkes, R. J., Cragg, B. A., & Raiswell, R. (2000): Isotopic evidence for anoxic pyrite oxidation and stimulation of bacterial sulphate reduction in marine sediments, *J. Geol. Soc. London*,157, 711–714. https://doi.org/10.1144/jgs.157.4.711.

Cabrol, L., Thalasso, F., Gandois, L., Sepulveda-Jauregui, A., Martinez-Cruz, K., Teisserenc, R., Tananaev, N., Tveit, A., Svenning, M. M., & Barret, M. (2020). Anaerobic oxidation of methane and associated microbiome in anoxic water of Northwestern Siberian lakes. *Science of the Total Environment*, *736*, 139588. https://doi.org/10.1016/j.scitotenv.2020.139588

Cai, C., Leu, A. O., Xie, G-J., Guo, J., Feng, Y., Zhao, J-X., Tyson, G. W., Yuan, Z., & Hu, S. (2018). A methanotrophic archaeon couples anaerobic oxidation of methane to Fe(II) reduction. ISME J, 12, 1929-1939. http://dx.doi.org/10.1038/s41396-018-0109-x

Cheng, L., Shi, S. bao, Yang, L., Zhang, Y., Dolfing, J., Sun, Y. ge, Liu, L., Li, Q., Tu, B., Dai, L., Shi, Q., & Zhang, H. (2019). Preferential degradation of long-chain alkyl substituted hydrocarbons in heavy oil under methanogenic conditions. *Organic Geochemistry*, *138*. https://doi.org/10.1016/j.orggeochem.2019.103927

Chuang, P. C., Yang, T. F., Wallmann, K., Matsumoto, R., Hu, C. Y., Chen, H. W., Lin, S., Sun, CH., Li, HC., Wang, Y., & Dale, A. W. (2019). Carbon isotope exchange during anaerobic oxidation of methane (AOM) in sediments of the northeastern South China Sea. *Geochimica et Cosmochimica Acta*, *246*, 138–155. https://doi.org/10.1016/j.gca.2018.11.003

Clement, J-C., Shrestha, J., Ehrenfeld, J. G., & Jaffe, P. R. (2005). Ammonium oxidation coupled to dissimilatory iron reduction under anaerobic conditions in wetland soils. *Soil biology and biochemistry, 37(12),* 2323-2328. http://doi.org/10.1016/j.soilbio.2005.03.027

Conrad, R. (2009). The global methane cycle: Recent advances in understanding the microbial processes involved. *Environmental Microbiology Reports*, *1*(5), 285–292. https://doi.org/10.1111/j.1758-2229.2009.00038.x

Crowe, S. A., Katsev, S., Leslie, K., Sturm, A., Magen, C., Nomosatryo, S., Pack, M. A., Kessler, J. D., Reeburgh, W. S., Roberts, J. a., González, L., Douglas Haffner, G., Mucci, A., Sundby, B., & Fowle, D. A. (2011). The methane cycle in ferruginous Lake Matano. *Geobiology, 9(1)*, 61-78. http://doi.org/10.1111/j.1472-4669.2010.00257.x

Damgaard, L. R., Revsbech, N. P., & Reichardt, W. (1998). Use of an oxygen-insensitive microscale biosensor for methane to measure methane concentration profiles in a rice paddy. *Applied and Environmental Microbiology, 64(3)*, 864-870. http://doi.org/10.1128/aem.64.3.864-870.1998

Dershwitz, P., Bandow, N. L., Yang, J., Semrau, J. D., McEllistrem, M. T., Heinze, R. A., Fonseca, M., Ledesma, J. C., Jennett, J. R., DiSpirito, A. M., Athwal, N. S., Hargrove, M. S., Bobik, T. A., Zischka, H., & DiSpirito, A. A. (2021). Oxygen Generation via Water Splitting by a Novel Biogenic Metal Ion-Binding Compound. *Applied and Environmental Microbiology*, *87*(14), 1–14. https://doi.org/10.1128/aem.00286-21

~~Eckert, T. (2000). The Influence of Chemical Stratification in the Water Column on Sulfur and Iron Dynamics in Pore Waters and Sediments of Lake Kinneret, Israel. *M.Sc. Thesis,* University of Bayreuth, Germany.~~

~~Egger, M., Rasigraf, O., Sapart, C.~~Ding, L. J., ~~Jilbert, T., Jetten, M.~~An, X. L., Li, S~~. M., Röckmann, T., van der Veen, C., Bândă, N., Kartal, B., Ettwig, K. F., & Slomp, C. P. (2015). Iron-mediated~~., Zhang, G. L., & Zhu, Y. G. (2014). Nitrogen loss through anaerobic ammonium oxidation ~~of methane in brackish coastal sediments.~~coupled to iron reduction from paddy soils in a chronosequence. *Environmental Science and Technology, ~~49~~(1), ~~277–283. https://doi.org/10.1021/es503663z~~48(18)*, 10641-10647. http://doi.org/10.1021/es503113s

Elul, M., Rubin-Blum, M., Ronen, Z., Bar-Or, I., Eckert, W., & Sivan, O. (2021). Metagenomic insights into the metabolism of microbial communities that mediate iron and methane cycling in Lake Kinneret sediments. *Biogeosciences Discussions*, 1–24. https://doi.org/10.5194/bg-2020-329

Elvert, M., Boetius, A., Knittel, K., & Jørgensen, B. B. (2003). Characterization of specific membrane fatty acids as chemotaxonomic markers for sulfate-reducing bacteria involved in anaerobic oxidation of methane. *Geomicrobiology Journal*, *20*(4), 403–419. https://doi.org/10.1080/01490450303894

Ettwig, K. F., Zhu, B., Speth, D., Keltjens, J. T., Jetten, M. S. M., & Kartal, B. (2016). Archaea catalyze iron-dependent anaerobic oxidation of methane. *PNAS, 113(45)*, 12792-12796. http://doi.org/10.1073/pnas.1609534113

Ettwig, Katharina F, Butler, M. K., Le Paslier, D., Pelletier, E., Mangenot, S., Kuypers, M. M. M., Schreiber, F., Dutilh, B. E., Zedelius, J., -de Beer, D. Gloerich, J., Wessels, H. J. C. T., van Alen, T., Luesken, F., Wu, M. L., van de Pas-Schoonen K. T., Op den Camp, H. J. M., Jansen-Megens, E. M., Francojs, KJ., Stunnenberg, H., Weissenbach, J., Jetten, M. S. M., & Strous, M. (2010). Nitrite-driven anaerobic methane oxidation by oxygenic bacteria. *Nature*, *464*(7288), 543–548. https://doi.org/10.1038/nature08883

Evans, P. N., Parks, D. H., Chadwick, G. L., Robbins, S, J., Orphan V. J., Golding, S. D., & Tyson, G. W. (2015). *Science*. 350(6259), 434-438. http://doi.org/ 10.1126/science.aac7745.

Fan, L., Dippold, M. A., Ge, T., Wu, J., Thiel, V., Kuzyakov, Y., & Dorodnikov, M. (2020). Anaerobic oxidation of methane in paddy soil: Role of electron acceptors and fertilization in mitigating CH4 fluxes. *Soil Biology and Biochemistry*, *141*, 107685. https://doi.org/10.1016/j.soilbio.2019.107685

Froelich, P. N., Klinkhammer, G. P., Lender, M. L., Luedtke, N. A., Heath, G. R., Cullen, D., Dauphin, P., Hammond, D., Hartman, B., & Maynard, V. (1979). *Geochemica et Cosmochimica Acta, 43*, 1075-1090. https://doi.org/10.1016/0016-7037(79)90095-4

Gropp, J., Iron, M. A., & Halevy, I. (2021). Theoretical estimates of equilibrium carbon and hydrogen isotope effects in microbial methane production and anaerobic oxidation of methane. *Geochimica et Cosmochimica Acta*, *295*, 237–264. https://doi.org/10.1016/j.gca.2020.10.018

~~Hadas, O., & Pinkas, R. (1995). Sulphate reduction in the hypolimnion and sediments of Lake Kinneret , Israel. *Freshwater Biology*, (33), 63–72.~~

Hallam, S. J., Putnam, N., Preston, C. M., Detter, J. C., Rokhsar, D., Richardson, P. H., & DeLong, E. F. (2004). Reverse methanogenesis: Testing the hypothesis with environmental genomics. *Science*, *305*(5689), 1457–1462. https://doi.org/10.1126/science.1100025

Hammer, Ø., Harper, D. A. T., & Ryan, P. D. (2001) Past: paleontological statistics software package for education and data analysis. *Paleontologia-Electronica*. 4 (1), 9.

Haroon, M. F., Hu, S., Shi, Y., Imelfort, M., Keller, J., Hugenholtz, P., Yuan, Z., & Tyson, G. W. (2013). Anaerobic oxidation of methane coupled to nitrate reduction in a novel archaeal lineage. *Nature*, *500*(7464), 567–570. https://doi.org/10.1038/nature12375

Hoehler, T. M., Alperin, M. J., Albert, D. B., & Martens, C. S. (1994). Field and laboratory, evidence for a methane-sulfate reducer consortium.pdf. *Global Biogeochemical Cycles*, *8*(4), 451–463.

Holler, T., Wegener, G., Niemann, H., Deusner, C., Ferdelman, T. G., Boetius, A., Brunner, B., & Widdel, F. (2011). Carbon and sulfur back flux during anaerobic microbial oxidation of methane and coupled sulfate reduction. *Proceedings of the National Academy of Sciences of the United States of America*, *108*(52). https://doi.org/10.1073/pnas.1106032108

Holmkvist, L., Ferdelman, T. G., & Jørgensen, B. B. (2011). A cryptic sulfur cycle driven by iron in the methane zone of marine sediment (Aarhus Bay, Denmark). *Geochimica et Cosmochimica Acta*, *75*(12), 3581–3599. https://doi.org/10.1016/j.gca.2011.03.033

Hug, L. A., Castelle, C. J., Wrighton, K. C., Thomas, B. C., Sharon, I., Frischkorn, K. R., Williams, K. H., Tringe, S. G., & Banfield, J. F. (2013). Community genomic analyses constrain the distribution of metabolic traits across the Chloroflexi phylum and indicate roles in sediment carbon cycling. *Microbiome*, *1*(1), 1–17. https://doi.org/10.1186/2049-2618-1-22

Kang, D. D., Li, F., Kirton, E., Thomas, A., Egan, R., An, H., & Wang, Z. (2019). MetaBAT 2: An adaptive binning algorithm for robust and efficient genome reconstruction from metagenome assemblies. *PeerJ*, *2019*(7), 1–13. https://doi.org/10.7717/peerj.7359

Kellermann, M. Y., Wegener, G., Elvert, M., Yoshinaga, M. Y., Lin, Y. S., Holler, T., Mollar, P. X., Knittel K.,

& Hinrichs, K. U. (2012). Autotrophy as a predominant mode of carbon fixation in anaerobic methane-oxidizing microbial communities. *Proceedings of the National Academy of Sciences of the USA* 109(47), 19321-19326. doi:10.1073/pnas.1208795109.

Kits, K. D., Klotz, M. G., & Stein, L. Y. (2015). Methane oxidation coupled to nitrate reduction under hypoxia by the Gammaproteobacterium Methylomonas denitrificans, sp. nov. type strain FJG1. *Environmental Microbiology*, *17*(9), 3219–3232. https://doi.org/10.1111/1462-2920.12772

Knittel, K., & Boetius, A. (2009). Anaerobic oxidation of methane: Progress with an unknown process. *Annual Review of Microbiology*, *63*, 311–334. https://doi.org/10.1146/annurev.micro.61.080706.093130

Kurth, J.M., Nadine T Smit, Stefanie Berger, Stefan Schouten, Mike S M Jetten, Cornelia U Welte, Anaerobic methanotrophic archaea of the ANME-2d clade feature lipid composition that differs from other ANME archaea, FEMS Microbiology Ecology, Volume 95, Issue 7, July 2019, fiz082.

Li, X., Hou, L., Liu, M., Zheng, Y., Yin, G., Lin, X., Cheng, L., Li, Y., & Hu, X. (2015). Evidence of Nitrogen Loss from Anaerobic Ammonium Oxidation Coupled with Ferric Iron Reduction in an Intertidal Wetland. *Environmental Science and Technology*, *49*(19), 11560–11568. https://doi.org/10.1021/acs.est.5b03419

Lin, Y. S., Lipp, J. S., Yoshinaga, M. Y., Lin, S. H., Elvert, M., & Hinrichs, K. U. (2010). Intramolecular stable carbon isotopic analysis of archaeal glycosyl tetraether lipids. *Rapid Communications in Mass Spectrometry*, *24*(19), 2817–2826. https://doi.org/10.1002/rcm.~~4707~~

~~Lovley~~4707Lovley, D. R., & Klug, M. J. (1983). Sulfate reducers can outcompete methanogens at freshwater sulfate concentrations. *Applied and Environmental Microbiology*, *45*(1), 187–192. https://doi.org/10.1128/aem.45.1.187-192.1983

~~Luo, J. H., Chen, H., Hu, S., Cai, C., Yuan, Z., & Guo, J. (2018). Microbial Selenate Reduction Driven by a Denitrifying Anaerobic Methane Oxidation Biofilm. *Environmental Science and Technology*, *52*(7), 4006–4012. https://doi.org/10.1021/acs.est.7b05046~~

Lovely, D. R., Coates, J. D., Blunt-Harris, E. L., Phillips, E. J. P., & Woodward, J. C. (1996). Humic substances as electron acceptors for microbial respiration. *Nature, 382*, 445-448. https://doi.org/10.1038/382445a0

Lu, Y. Z., Fu, L., Ding, J., Ding, Z. W., Li, N., & Zeng, R. J. (2016). Cr(VI) reduction coupled with anaerobic oxidation of methane in a laboratory reactor. *Water Research, 102*, 445-452. http://doi.org/10.1016/j.watres.2016.06.065

Martinez-cruz, K., Leewis, M., Charold, I., Sepulveda-jauregui, A., Walter, K., Thalasso, F., & Beth, M. (2017). Science of the Total Environment Anaerobic oxidation of methane by aerobic methanotrophs in sub-Arctic lake sediments. *Science of the Total Environment*, *607–608*, 23–31. https://doi.org/10.1016/j.scitotenv.2017.06.187

Meador, T. B., Gagen, E. J., Loscar, M. E., Goldhammer, T., Yoshinaga, M. Y., Wendt, J., Thomm, M., & Hinrichs, K. U. (2014). Thermococcus kodakarensis modulates its polar membrane lipids and elemental composition according to growth stage and phosphate availability. *Frontiers in Microbiology*, *5*(JAN), 1–

13. https://doi.org/10.3389/fmicb.2014.00010

Meister, P., Liu, B., Khalili, A., Böttcher, M. E., & Jørgensen, B. B. (2019). Factors controlling the carbon isotope composition of dissolved inorganic carbon and methane in marine porewater: An evaluation by reaction-transport modelling. *Journal of Marine Systems*, *200*(August), 103227. https://doi.org/10.1016/j.jmarsys.2019.103227

Moran, J. J., House, C. H., Freeman, K. H., & Ferry, J. G. (2005). Trace methane oxidation studied in several Euryarchaeota under diverse conditions. *Archaea*, *1*(5), 303–309. https://doi.org/10.1155/2005/650670

Mosrovaya, A., Wind-Hansen, M., Rousteau, P., Bristow, L. A., & Thamdrup, B. (2021) Sulfate- and iron-dependent anaerobic methane oxidation occuring side-by-side in freshwater lake sediments. *Limnology and Oceanography*. https://doi.org/10.1002/lno.11988

Nollet, L., Demeyer, D., & Verstraete, W. (1997). Effect of 2-bromoethanesulfonic acid and Peptostreptococcus productus ATCC 35244 addition on stimulation of reductive acetogenesis in the ruminal ecosystem by selective inhibition of methanogenesis. *Applied and Environmental Microbiology*, *63*(1), 194–200. https://doi.org/10.1128/aem.63.1.194-200.1997

Norði, K á., Thamdrup B., & Schubert, C. J. (2013). Anaerobic oxidation of methane in an iron-rich Danish freshwater lake sediment. *Limnology and Oceanography, 58(2)*, 546-554. http://doi.org/10.4319/lo.2013.58.2.0546

Norði, K á., & Thamdrup B. (2014). Nitrate-dependent anaerobic methane oxidation in freshwater sediment. *Geochimica et Cosmochimica Acta, 132*, 141-150. http://doi.org/10.1016/j.gca.2014.01.032

Nurk, S., Bankevich, A., & Antipov, D. (2013). Assembling genomes and mini-metagenomes from highly chimeric reads. *Research in Computational Molecular Biology*, 158–170. https://doi.org/10.1007/978-3-642-37195-0

Nüsslein, B., Chin, K. J., Eckert, W., & Conrad, R. (2001). Evidence for anaerobic syntrophic acetate oxidation during methane production in the profundal sediment of subtropical Lake Kinneret (Israel). *Environmental Microbiology*, *3*(7), 460–470. https://doi.org/10.1046/j.1462-2920.2001.00215.x

Orembland, R. S., & Capone, D. G. (1988). *Use of "Specific" Inhibitors in Biogeochemistry and Microbial Ecology* (Vol. 10). https://doi.org/10.2307/4514

Orphan, V. J., House, C. H., & Hinrichs, K. (2001). Methane-Consuming Archaea Revealed by Directly Coupled Isotopic and Phylogenetic Analysis. *Science*, *293*(July), 484–488. https://doi.org/10.1126/science.1061338

Oswald, K., Milucka, J., Brand, A., Hach, P., Littmann, S., Wehrli, B., Albersten, M., Daims, H., Wagner, M., Kuypers, M. M. M., Schubert, C. J., & Milucka, J. (2016). Aerobic gammaproteobacterial methanotrophs mitigate methane emissions from oxic and anoxic lake waters. *Limnology and Oceanography*, *61*, S101–S118. https://doi.org/10.1002/lno.10312

Parks, D. H., Chuvochina, M., Rinke, C., Mussig, A. J., Chaumeil, P-A., & Hugenholtz, P. (2021) GTDB: an

ongoing census of bacterial and archaeal diversity through a phylogenetically consistent, rank normalized and complete genome-based taxonomy. *Nucleic Acids Research, 202, 1-10.* http://doi.org/10.1093/nar/gkab776

Raghoebarsing, A. A., Pol, A., Van De Pas-Schoonen, K. T., Smolders, A. J. P., Ettwig, K. F., Rijpstra, W. I. C., Schouten, S., Sinninghe Damsté, J. S., Op den Camp, H. J. M., Jetten, M. S. M., & Strous, M. (2006). A microbial consortium couples anaerobic methane oxidation to denitrification. *Nature*, *440*(7086), 918–921. https://doi.org/10.1038/nature04617

Reeburgh, W. S. (2007). Oceanic Methane Biogeochemistry. *ChemInform*, *38*(20), 486–513. https://doi.org/10.1002/chin.200720267

Rosentreter, J. A., Borges, A. V., Deemer, B. R., Holgerson, M. A., Liu, S., Song, C., Melack, J., Raymond, P. A., Duarte, C. M., Allen, G. H., Olefeldt, D., Poulter, B., Battin, T. I., & Eyre, B. D. (2021). *Nature geoscience, 14(4)*, 225-230. http://doi.org/ 10.1038/s41561-021-00715-2

Saunois, M., Stavert, A. R., Poulter, B., Bousquet, P., Canadell, J. G., Jackson, R. B., Raymond, P. A., Dlugokencky, E. J., Houweling, S., Patra, P. K., Ciais, P., Arora, V. K., Bastviken, D., Bergamaschi, P., Blake, D. R., Brailsford, G., Bruhwiler, L., Carlson, K. M., Carrol, M., Castaldi, S., Chandra, N., Crevoisier, C., Crill, P. M., Covey, K., Curry, C. L., Etiope, G., Frankenberg, C., Gedney, N., Hegglin, M. I., Höglund-Isaksson, L., Hugelius, G., Ishizawa, M., Ito, A., Janssens-Maenhout, G., Jensen, K. M., Joos, F., Kleinen, T., Krummel, P. B., Langenfelds, R. L., Laruelle, G. G., Liu, L., Machida, T., Maksyutov, S., McDonald, K. C., McNorton, J., Miller, P. A., Melton, J. R., Morino, I., Müller, J., Murguia-Flores, F., Naik, V., Niwa, Y., Noce, S., O'Doherty, S., Parker, R. J., Peng, C., Peng, S., Peters, G. P., Prigent, C., Prinn, R., Ramonet, M., Regnier, P., Riley, W. J., Rosentreter, J. A., Segers, A., Simpson, I. J., Shi, H., Smith, S. J., Steele, L. P., Thornton, B. F., Tian, H., Tohjima, Y., Tubiello, F. N., Tsuruta, A., Viovy, N., Voulgarakis, A., Weber, T. S., van Weele, M., van der Werf, G. R., Weiss, R. F., Worthy, D., Wunch, D., Yin, Y., Yoshida, Y., Zhang, W., Zhang, Z., Zhao, Y., Zheng, B., Zhu, Q., Zhu, Q., and Zhuang, Q.: The Global Methane Budget 2000–2017, Earth Syst. Sci. Data, 12, 1561–1623, https://doi.org/10.5194/essd-12-1561-2020, 2020.

~~Scheller, S., Yu, H., Chadwick, G. L., McGlynn, S. E., & Orphan, V. J. (2016). Artificial electron acceptors decouple archaeal methane oxidation from sulfate reduction. *Science*, *351*(6274), 1754–1756. https://doi.org/10.1126/science.aad7154~~

~~Segarra, K. E. a, Comerford~~Schubert, C~~., Slaughter, J., & Joye, S. B. (2013). Impact of electron acceptor availability on the~~. J., Vazquez, F., Lösekann-Behrens, T., Knittel, K., Tonolla, M., & Boetius, A. (2011). Evidence for anaerobic oxidation of methane in ~~coastal~~sediments of a freshwater ~~and brackish wetland sediments. *Geochimica et Cosmochimica Acta*, *115*, 15–30. https://~~system (Lago di Cadagno). *FEMS Microbiology Ecology, 76(1)*, 26-38. http://doi.org/ 10.1111/j.1574-6941.2010.01036.x

Segarra, K. E. A., Schubotz, F., Samarkin, V., Yoshinaga, M. Y., Hinrichs, K-U., & Joye, S. B. (2015). *Nature communications, 6(may)*, 1-8. http://dx.doi.org/10.~~1016/j.gca.2013.03.029~~1038/ncomms8477

Sela-Adler, M., Herut, B., Bar-Or, I., Antler, G., Eliani-Russak, E., Levy, E., Makovsky, Y., & Sivan, O. (2015). Geochemical evidence for biogenic methane production and consumption in the shallow

sediments of the SE Mediterranean shelf (Israel). *Continental Shelf Research*, *101*, 117–124. https://doi.org/10.1016/j.csr.2015.04.001

Serruya, C. (1971). Lake Kinneret: the nutrient chemistry of the Sediments. *Limnology and Oceanography*, *16*(May), 510–521.

Shrestha, J., Rich, J. J., Ehrenfeld, J. G., & Jaffe, P. R. (2009). Oxidation of ammonium to nitrite under iron-reducing conditions in wetland soils: Laboratory, field demonstrations, and push-pull rate determination. *Soil Science, 174(3)*, 156-164. http://doi.org/10.1097/SS.0b013e3181988fbf

Shuai, W., & Jaffé, P. R. (2019). Anaerobic ammonium oxidation coupled to iron reduction in constructed wetland mesocosms. *Science of the Total Environment*, *648*, 984–992. https://doi.org/10.1016/j.scitotenv.2018.08.189

Sieber, C. M. K., Probst, A. J., Sharrar, A., Thomas, B. C., Hess, M., Tringe, S. G., & Banfield, J. F. (2018). Recovery of genomes from metagenomes via a dereplication, aggregation and scoring strategy. *Nature Microbiology*, *3*(7), 836–843. https://doi.org/10.1038/s41564-018-0171-1

Sinke, A. J.C., Cornelese, A. A., Cappenberg, T. E., & Zehnder, A. J. B. (1992). Seasonal variation in sulfate reduction and methanogenesis in peaty sediments of eutrophic Lake Loosdrecht, The Netherlands. *Biogeochemistry, 16(1)*, 43-61. http://doi.org/10.1007/BF02402262

Sivan, O, Adler, M., Pearson, A., Gelman, F., Bar-Or, I., John, S. G., & Eckert, W. (2011). Geochemical evidence for iron-mediated anaerobic oxidation of methane. *Limnology and Oceanography*, *56*(4), 1536–1544.

Sivan, O., Antler, G., Turchyn, A. V., Marlow, J. J., & Orphan, V. J., (2014). Iron oxides stimulate sulfate-driven anaerobic methane oxidation in seeps. PNAS. 111, E4139-E4147. http://doi.org/10.1073/pnas.1412269111

Sivan, O., Shusta, S., & Valentine, D. L. (2016). Methanogens rapidly transition from methane production to iron reduction. *Geobiology*, 190–203. https://doi.org/10.1111/gbi.12172

Stookey, L. L. (1970). Ferrozine-a new spectrophotometric reagent for iron. *Analytical Chemistry*, *42*(7), 779–781. https://doi.org/10.1021/ac60289a016

Sturt, H. F., Summons, R. E., Smith, K., Elvert, M., & Hinrichs, K. U. (2004). Intact polar membrane lipids in prokaryotes and sediments deciphered by high-performance liquid chromatography/electrospray ionization multistage mass spectrometry - New biomarkers for biogeochemistry and microbial ecology. *Rapid Communications in Mass Spectrometry*, *18*(6), 617–628. https://doi.org/10.1002/rcm.1378

Su, G., Zopfi, J., Yao, H., Steinle, L., Niemann, H., & Lehmann, M. F. (2020). Manganese/iron-supported sulfate-dependent anaerobic oxidation of methane by archaea in lake sediments. *Limnology and Oceanography*, *65*(4), 863–875. https://doi.org/10.1002/lno.11354

Tamames, J., & Puente-Sánchez, F. (2019). SqueezeMeta, A Highly Portable, Fully Automatic Metagenomic Analysis Pipeline. *Frontiers in Microbiology*, *9*. https://doi.org/10.3389/fmicb.2018.03349

Tan, X., Xie, G. J., Nie, W. B., Xing, D-F., Liu, B. F., Ding, J., & Ren, N. Q. (2021). Fe(III)-mediated anaerobic ammonium oxidation: A novel microbial nitrogen cycle pathway and potential applications. *Critical Reviews in Environmental Science and Technology*. https://doi.org/10.1080/10643389.2021.1903788

Timmers, P. H. A., Welte, C. U., Koehorst, J. J., Plugge, C. M., Jetten, M. S. M., & Stams, A. J. M. (2017). Reverse Methanogenesis and Respiration in Methanotrophic Archaea. *Archaea*, *2017*(Figure 1). https://doi.org/10.1155/2017/1654237

Treude, T., Krause, S., Maltby, J., Dale, A. W., Coffin, R., & Hamdan, L. J. (2014). Sulfate reduction and methane oxidation activity below the sulfate-methane transition zone in Alaskan Beaufort Sea continental margin sediments: Implications for deep sulfur cycling. *Geochimica et Cosmochimica Acta*, *144*, 217–237. https://doi.org/10.1016/j.gca.2014.08.018

Treude, T., Niggemann, J., Kallmeyer, J., Wintersteller, P., Schubert, C. J., Boetius, A., & Jørgensen, B. B. (2005). Anaerobic oxidation of methane and sulfate reduction along the Chilean continental margin. *Geochimica et Cosmochimica Acta*, *69*(11), 2767–2779. https://doi.org/10.1016/j.gca.2005.01.002

Valentine D. L. (2002). Biogeochemistry and microbial ecology of methane oxidation in anoxic environments: A review. Antonie van Leeuwenhoek, 81(1-4), 271-282. http://doi.org/ 10.1023/A:1020587206351

Valenzuela, E. I., Avendaño, K. A., Balagurusamy, N., Arriaga, S., Nieto-Delgado, C., Thalasso, F., & Cervantes, F. J. (2019). Electron shuttling mediated by humic substances fuels anaerobic methane oxidation and carbon burial in wetland sediments. *Science of the Total Environment*, *650*, 2674–2684. https://doi.org/10.1016/j.scitotenv.2018.09.388

Valenzuela, E. I., Prieto-Davó, A., López-Lozano, N. E., Hernández-Eligio, A., Vega-Alvarado, L., Juárez, K., García-González, A. S., López, M. G., & Cervantes, F. J. (2017). Anaerobic methane oxidation driven by microbial reduction of natural organic matter in a tropical wetland. *Applied and Environmental Microbiology*, *83*(11), 1–15. https://doi.org/10.1128/AEM.00645-17

Vigderovich, H., Liang, L., Herut, B., Wang, F., Wurgaft, E., Rubin-Blum, M., & Sivan, O. (2019). Evidence for microbial iron reduction in the methanogenic sediments of the oligotrophic SE Mediterranean continental shelf. *Biogeosciences Discussions*, 1–25. https://doi.org/10.5194/bg-2019-21

Wang, L., Miao, X., Ali, J., Lyu, T., & Pan, G. (2018). Quantification of Oxygen Nanobubbles in Particulate Matters and Potential Applications in Remediation of Anaerobic Environment. *ACS Omega*, *3*(9), 10624–10630. https://doi.org/10.1021/acsomega.8b00784

Wegener G, Niemann H, Elvert M, Hinrichs K-U, Boetius A (2008). Assimilation of methane and inorganic carbon by microbial communities mediating the anaerobic oxidation of methane. Environmental Microbiology 10(9), 2287-2298. doi: 10.1111/j.1462-2920.2008.01653.x.

Wegener, G., Gropp, J., Taubner, H., Halevy, I., & Elvert, M. (2021). Sulfate-dependent reversibility of intracellular reactions explains the opposing isotope effects in the anaerobic oxidation of methane. *Science Advances*, *7*(19), 1–14. https://doi.org/10.1126/sciadv.abe4939

Whiticar, M. J., Faber, E., & Schoell, M. (1986). Biogenic methane formation in marine and freshwater environments: CO2 reduction vs. acetate fermentation-Isotope evidence. Geochimica et Cosmochimica Acta, 50(5), 693-709. http://doi.org/ 10.1016/0016-7037(86)90346-7

Wu, Y.W., Tang, Y.-H., Tringe, S. G., Simmons, B. A., & Singer, S. W. (2014). MaxBin: an automated binning method to recover individual genomes from metagenomes using. *Microbiome*, *2*(26), 4904–4909. Retrieved from https://microbiomejournal.biomedcentral.com/articles/10.1186/2049-2618-2-26

Wuebbles, D. J., & Hayhoe, K. (2002). Atmospheric methane and global change. *Earth-Science Reviews*, *57*(3–4), 177–210. https://doi.org/10.1016/S0012-8252(01)00062-9

Xu, Z., Masuda, Y., Wang, X., Ushijima, N., Shiratori, Y., Senoo, K., & Itoh, H. (2021). Genome-Based Taxonomic Rearrangement of the Order Geobacterales Including the Description of Geomonas azotofigens sp. nov. and Geomonas diazotrophica sp. nov. Frontiers in Microbiology, 12(September). http://doi.org/ 10.3389/fmicb.2021.737531

Yorshansky, O. (2019). *Iron Reduction in Deep Marine Sediments of the Eastern Mediterranean Continental Shelf and the Yarqon Estuary*. MsC thesis, Ben Gurion University of the Negev.

Yoshinaga, M. Y., Holler, T., Goldhammer, T., Wegener, G., Pohlman, J. W., Brunner, B., Kuypers, M. M. M., Hinrichs, K. U., & Elvert, M. (2014). Carbon isotope equilibration during sulphate-limited anaerobic oxidation of methane. *Nature Geoscience*, *7*(3), 190–194. https://doi.org/10.1038/ngeo2069

Zehnder, -a J., & Brock, T. D. (1979). Methane formation and methane oxidation by methanogenic bacteria. *Journal of Bacteriology*, *137*(1), 420–432.

Zhang, X., Xia, J., Pu, J., Cai, C., Tyson, G. W., Yuan, Z., & Hu, S. (2019). Biochar-Mediated Anaerobic Oxidation of Methane. *Environmental Science and Technology*, *53*(12), 6660–6668. https://doi.org/10.1021/acs.est.9b01345

Zheng, Y., Wang, H., Liu, Y., Zhu, B., Li, J., Yang, Y., Qin, W., Chen, L., Wu, X., Chistoserdova, L., & Zhao, F. (2020). Methane-Dependent Mineral Reduction by Aerobic Methanotrophs under Hypoxia. *Environmental Science and Technology Letters*, *7*(8), 606–612. https://doi.org/10.1021/acs.estlett.0c00436